

AD-A088 917

BELL HELICOPTER TEXTRON FORT WORTH TX

F/6 2 /11

INVESTIGATION OF VIBRATION REDUCTION THROUGH STRUCTURAL OPTIMIZ-- TC(U)

JUL 80 H W HANSON

DAAK51-78-C-0011

UNCLASSIFIED

699-099-122

USAAVRADCOM-TR-80-D-13

NL

1 of 1
40 A
0004 7

END
DATE
FILMED
10-80
DTIC

USAAVRADCOM-TR-80-D-13

AD A088917

INVESTIGATION OF VIBRATION REDUCTION THROUGH
STRUCTURAL OPTIMIZATION

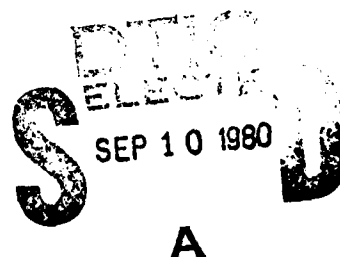
H. W. Hanson
BELL HELICOPTER TEXTRON
P. O. Box 482
Fort Worth, Tex. 76101

July 1980

Final Report for Period August 1978 - March 1980

Approved for public release;
distribution unlimited.

THIS DOCUMENT IS BEST QUALITY PRACTICABLE.
THE COPY FURNISHED TO DDC CONTAINED A
SIGNIFICANT NUMBER OF PAGES WHICH DO NOT
REPRODUCE LEGIBLY.



Prepared for

APPLIED TECHNOLOGY LABORATORY

U. S. ARMY RESEARCH AND TECHNOLOGY LABORATORIES (AVRADCOM)

Fort Eustis, Va. 23604

DDC FILE COPY

80 9 10 036

APPLIED TECHNOLOGY LABORATORY POSITION STATEMENT

In the area of aircraft structural dynamic design, the existence of a reliable structural optimization method can be a valuable design tool, enabling a designer to perform rapid identification and evaluation of the most promising structural elements, which, upon modification of their modal properties, could minimize vibration response. In this program, a feasibility study was performed to evaluate two structural optimization methods, the Vincent circle and the forced response strain energy method for reducing vibration response, primarily via structural stiffness changes, using NASTRAN beam-element representation of the AH-1G with uniform damping. The forcing function consisted of a single main rotor 2 rev steady-state vertical excitation. The pilot's seat was selected as the location for dynamic response reduction.

The relative effectiveness of the methods to minimize the dynamic response at the selected location, subject to the constraints and considerations stated above, was based essentially on two factors: (a) selection of practical stiffness changes that an element can undergo, and (b) evaluation of the effectiveness of the groups of elements predicted by each method by calculating the response of the structure subject to practical stiffness changes.

The results obtained from the two methods, i.e., stiffness changes required and group of elements identified with high potential for reducing vibration, at best, do not agree. These results indicate that the forced response strain energy method is more suitable in attaining response reduction according to the investigative methodology used in this program.

The Vincent circle method was further investigated in conjunction with mass and damping changes. Also, the possibility that the Vincent circle method would indicate the optimum location of a fixed mass and damping dynamic absorber was investigated, yielding negative results.

The project engineer for this effort was Mr. N. J. Calapodas of the Aeronautical Technology Division, Structures Technical Area.

DISCLAIMERS

The findings in this report are not to be construed as an official Department of the Army position unless so designated by other authorized documents.

When Government drawings, specifications, or other data are used for any purpose other than in connection with a definitely related Government procurement operation, the United States Government thereby incurs no responsibility nor any obligation whatsoever; and the fact that the Government may have formulated, furnished, or in any way supplied the said drawings, specifications, or other data is not to be regarded by implication or otherwise as in any manner licensing the holder or any other person or corporation, or conveying any rights or permission, to manufacture, use, or sell any patented invention that may in any way be related thereto.

Trade names cited in this report do not constitute an official endorsement or approval of the use of such commercial hardware or software.

DISPOSITION INSTRUCTIONS

Destroy this report when no longer needed. Do not return it to the originator.

DISCLAIMER NOTICE

**THIS DOCUMENT IS BEST QUALITY
PRACTICABLE. THE COPY FURNISHED
TO DTIC CONTAINED A SIGNIFICANT
NUMBER OF PAGES WHICH DO NOT
REPRODUCE LEGIBLY.**

UNCLASSIFIED (19)
SECURITY CLASSIFICATION OF THIS PAGE (When Data Entered)

REPORT DOCUMENTATION PAGE		READ INSTRUCTIONS BEFORE COMPLETING FORM
1. REPORT NUMBER USAAVRADCOM TR-80-D-13	2. GOVT ACCESSION NO. AD-A088917	3. RECIPIENT'S CATALOG NUMBER
4. TITLE (and Subtitle) INVESTIGATION OF VIBRATION REDUCTION THROUGH STRUCTURAL OPTIMIZATION		5. FUNDING NUMBERS Final Report August 1978 - March 1980
6. AUTHOR(s) Horace W. Hanson		7. PERFORMING ORG. REPORT NUMBER 699-099-1224
8. AUTHORING OR GRANT NUMBER(s) DAAK51-78-C-6011		9. PROGRAM ELEMENT, PROJECT, TASK AND MONITORING ORG. NUMBERS 62209A/1L1622/9AH76
10. PERFORMING ORGANIZATION NAME AND ADDRESS Bell Helicopter Textron P.O. Box 482 Fort Worth, Texas 76101		11. REPORT DATE July 1980
12. CONTROLLING OFFICE NAME AND ADDRESS Applied Technology Laboratory, U.S. Army Research & Technology Laboratories (AVRADCOM), Fort Eustis, Virginia 23604		13. NUMBER OF PAGES 93
14. MONITORING AGENCY NAME & ADDRESS (if different from Controlling Office) 1296		15. SECURITY CLASS. (of this report) Unclassified
16. DISTRIBUTION STATEMENT (of this Report) Approved for public release; distribution unlimited.		15a. DECLASSIFICATION/DOWNGRADING SCHEDULE
17. DISTRIBUTION STATEMENT (of the abstract entered in Block 20, if different from Report)		
18. SUPPLEMENTARY NOTES		
19. KEY WORDS (Continue on reverse side if necessary and identify by block number) Helicopter Optimization Forced response Dynamic Vincent circle Modal Vibration NASTRAN Structure Strain energy		
20. ABSTRACT (Continue on reverse side if necessary and identify by block number) The purpose of this program was to investigate structural optimization techniques for vibration reduction. The results of a practical evaluation of two such techniques, the Vincent circle method and the forced response strain energy method, are discussed. Initial comparison studies of the two methods based on stiffness parameter variations were conducted using an elastic-line NASTRAN		

(continued)

DD FORM 1 JAN 73 1473 EDITION OF 1 NOV 65 IS OBSOLETE

UNCLASSIFIED
SECURITY CLASSIFICATION OF THIS PAGE (When Data Entered)

054200 Jm

UNCLASSIFIED

SECURITY CLASSIFICATION OF THIS PAGE(When Data Entered)

model of the AH-1G helicopter. The forced response strain energy method was then applied to a large complex built-up NASTRAN AH-1G model. This application provided useful comparative data identifying the structural elements considered to be the primary contributors to the response. Realistic structural stiffness changes in these elements were assessed to determine their effect on vibration reduction. The Vincent circle method was further evaluated for mass tuning, damping, and dynamic absorber parameters using the elastic-line model.

UNCLASSIFIED

SECURITY CLASSIFICATION OF THIS PAGE(When Data Entered)

PREFACE

This investigation of vibration reduction through structural optimization was performed under Contract DAAK51-78-C-0011 for the Applied Technology Laboratory, U. S. Army Research and Technology Laboratories (AVRADCOM), Fort Eustis, Virginia. The program was implemented under the technical direction of Mr. Nicholas J. Calapodas of the Applied Technology Laboratory.

A literature survey of structural optimization techniques for vibration reduction was performed and two techniques - the Vincent circle method and the forced response strain energy method - were evaluated using a NASTRAN analysis of the Model AH-1G helicopter. Mr. Horace W. Hanson was the Bell Helicopter Textron Project Engineer.

Accession For	
NTIS Cover	<input checked="checked" type="checkbox"/>
DDC Tag	<input type="checkbox"/>
Unprocessed	<input type="checkbox"/>
Justification	
Distribution/	
Availability Codes	
Avail and/or	
Special	
Dist.	
A	230

TABLE OF CONTENTS

	<u>Page</u>
PREFACE	3
LIST OF ILLUSTRATIONS	6
LIST OF TABLES	8
INTRODUCTION	9
LITERATURE SURVEY	10
STRUCTURAL OPTIMIZATION METHODS UNDER EVALUATION	12
VINCENT CIRCLE METHOD	12
STRAIN ENERGY METHOD	15
Modal Strain Energy Approach	15
Forced Response Strain Energy Approach	16
PROGRAM OBJECTIVES	18
ANALYTICAL APPROACH	19
METHOD OF ANALYSIS	19
MATHEMATICAL MODELS	21
PRACTICAL CRITERION FOR STRUCTURAL STIFFNESS CHANGES	26
STIFFNESS PARAMETER INVESTIGATIONS	27
ELASTIC-LINE MODEL ANALYSIS	27
Forced Response Strain Energy Results	27
Vincent Circle Results	27
Strain Energy/Vincent Circle Comparison	35
BUILT-UP MODEL VIBRATION OPTIMIZATION	39
FURTHER EVALUATION OF THE VINCENT CIRCLE	46
MASS PARAMETER RESULTS	46
DAMPING PARAMETER RESULTS	46
DYNAMIC ABSORBER PARAMETER RESULTS	46
CONCLUSIONS	51
REFERENCES	52
APPENDIX A - AH-1G ELASTIC-LINE NASTRAN MODEL	54
APPENDIX B - NASTRAN FORCED RESPONSE STRAIN ENERGY OUTPUT DATA	58
SYMBOLS	92

LIST OF ILLUSTRATIONS

<u>Figure</u>		<u>Page</u>
1	Vincent circle phenomenon	13
2	Boeing-Vertol CH-47A vibration reduction by structural modification	17
3	AH-1G elastic-line math model	22
4	Elastic-line model main rotor pylon	23
5	AH-1G built-up math model	24
6	Elastic-line model 2/rev forced response mode shape	28
7	Elastic-line model forced response strain energy distribution	29
8	Vincent circle plot for upper main rotor mast segment	31
9	Vincent circle plots for aft fuselage segment	32
10	Elastic-line model Vincent circle diameter distribution for pilot's seat response	33
11	Elastic-line model optimum pilot's seat vibration reduction based on Vincent circle properties	34
12	Typical sensitivity of Vincent circle response region	37
13	Forced response strain energy comparison to Vincent circle	38
14	Built-up model 2/rev forced response mode shape ...	40
15	Comparison of forced response strain energy distributions	41
16	Simplified built-up model forced response mode shapes showing vibration optimization process	44
17	Typical Vincent circle stiffness/mass response region relationships	47

LIST OF ILLUSTRATIONS - Concluded

<u>Figure</u>		<u>Page</u>
18	Effect of damping on typical Vincent circle response region	48
19	Comparison of Vincent circle properties to dynamic absorber location effectiveness for reducing pilot's seat vibration	49

LIST OF TABLES

<u>Table</u>		<u>Page</u>
1	AH-1G model comparison	25
2	Elastic-line model element stiffness values for minimum and maximum pilot's seat response	36
3	Built-up model pilot's seat vibration reduction	43

INTRODUCTION

In the development of a helicopter airframe structure, part of the design cycle must be concerned with keeping vibration to a minimum. The analysis and control of helicopter airframe dynamic characteristics are quite complex. The reasons are, in part:

- The large number of main rotor harmonic excitations simultaneously present, as well as excitations from secondary sources such as the tail rotor and shafting.
- The large variation in main rotor oscillatory hub forces and moments and phase relationships as a function of ship gross weight and center-of-gravity, airspeed, temperature, altitude, etc.
- The large number of locations at which vibrations must be controlled within the aircraft for reasons of crew and passenger comfort, system reliability, and service life of the airframe structure and components.
- Design changes for vibration control that must be accomplished within the framework of the overall design criteria, including many considerations such as size, strength, weight, and aerodynamic drag.

Vibration reduction is primarily accomplished through dynamic devices such as vibration isolation systems and dynamic absorbers, and/or through structural modifications that improve the vibratory elastic deformation characteristics of the airframe. Rapid and efficient techniques are needed for evaluating and optimizing these structural changes to minimize the vibration response. Two methods of reducing vibration through structural optimization were evaluated in this study - the Vincent circle method and the forced response strain energy method.

LITERATURE SURVEY

A brief search was conducted to locate and review existing literature applicable to vibration reduction by structural optimization techniques with emphasis on the Vincent circle and the forced response strain energy methods. Three data bases were used in the survey:

- The National Technical Information Service (NTIS)
- The Defense Technical Information Center (DTIC)
- The Engineering Index (COMPENDEX)

The information that is cataloged in the National Technical Information Service is derived from publications of the federal, state, and local government agencies; private industry; and universities, with emphasis placed on commercial applications. The information available from DTIC is obtained from many of the same sources as NTIS; however, the emphasis is placed on military and defense usage. The Engineering Index contains publications of the engineering societies, such as the proceedings of conferences, journals, and magazines.

Five documents applicable to the Vincent circle method were found (References 1 through 5). Only one report addressing

¹Vincent, A. H., A NOTE ON THE PROPERTIES OF THE VARIATION OF STRUCTURAL RESPONSE WITH RESPECT TO A SINGLE STRUCTURAL PARAMETER WHEN PLOTTED IN THE COMPLEX PLANE, Westland Helicopters Limited Report GEN/DYN/RES/010R, Yeovil, Somerset, England, September 1973.

²Done, G. T. S., and Hughes, A. D., THE RESPONSE OF A VIBRATING STRUCTURE AS A FUNCTION OF STRUCTURAL PARAMETERS, Journal of Sound and Vibration, Vol. 38, No. 2, 1975, pp. 255-266.

³Done, G. T. S., and Hughes, A. D., REDUCING VIBRATION BY STRUCTURAL MODIFICATION, Vertica, Vol. 1, No. 1, 1976, pp. 31-38, (paper presented at the First European Rotorcraft and Powered Lift Aircraft Forum at Southampton, September 22-24, 1975).

⁴Done, G. T. S., Hughes, A. D., and Webby, J., THE RESPONSE OF A VIBRATING STRUCTURE AS A FUNCTION OF STRUCTURAL PARAMETERS - APPLICATION AND EXPERIMENT, Journal of Sound and Vibration, Vol. 49, No. 2, 1976, pp. 149-159.

⁵Balmford, D. E. H., THE CONTROL OF VIBRATION IN HELICOPTERS, Aeronautical Journal, Vol. 81, No. 794, February 1977, pp. 63-67.

the forced response strain energy method was located (Reference 6).

The search did not disclose any other literature that dealt specifically with vibration reduction through structural optimization.

⁶Sciarra, J. J., USE OF THE FINITE ELEMENT DAMPED FORCED RESPONSE STRAIN ENERGY DISTRIBUTION FOR VIBRATION REDUCTION, Boeing-Vertol Company Report D210-10819-1, U.S. Army Research Office - Durham, Durham, North Carolina, July, 1974.

STRUCTURAL OPTIMIZATION METHODS UNDER EVALUATION

VINCENT CIRCLE METHOD

If a damped linear structure is excited by a constant sinusoidal force at a single location, the response of some other point in the structure can be shown to trace out a circular locus in the complex plane when any single structural element stiffness or mass parameter is continuously varied from minus infinity to plus infinity, as illustrated in Figure 1. This dynamic property of linear structures is known as the Vincent circle phenomenon (Reference 1). The phenomenon requires that some value of damping be present in order to develop the imaginary component of the response. The minimum response attainable, due to a particular stiffness or mass parameter, is indicated by the radius of the response circle and location of its center. Use of these circular properties will hereafter be referred to as the Vincent circle method.

The relevant mathematics of this circular response phenomenon, based on the theory originally established by Vincent, are given by Done and Hughes (Reference 2) and are summarized as follows:

The structure shown in Figure 1 has many degrees-of-freedom, and the response at point q due to a single sinusoidal force at point p is being examined. The amplitude of the displacement response vector, x , for the structure is given by

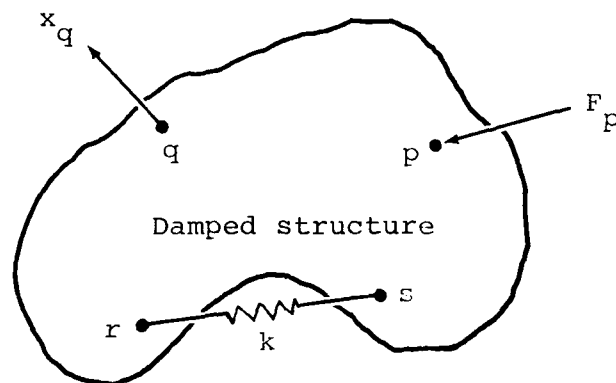
$$x = GF \quad (1)$$

where

$$G = [K - M\omega^2 + i\omega C]^{-1} \quad (2)$$

Consider two points, r and s, in the structure having mutually compatible degrees of freedom. A linear spring of stiffness, k , is inserted between these two points so as to exert zero force when the original structure is in equilibrium. Considering the structure as a free body, the forces exerted on it at points r and s by the spring are F_r and F_s , respectively, which have the relationship

$$F_r = k(x_s - x_r) = -F_s \quad (3)$$



Apply constant sinusoidal force of amplitude F at point p , vary spring stiffness k between points r and s , and measure response x at point q .

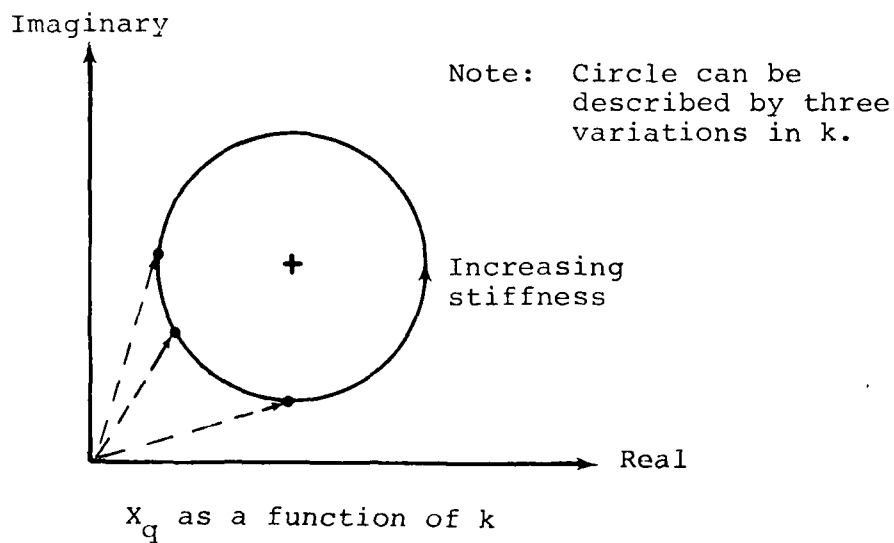


Figure 1. Vincent circle phenomenon.

The nonzero elements in the forcing vector F are F_r , F_s , and F_p . The response equations of interest are

$$x_q = G_{qp} F_p + G_{qr} F_r + G_{qs} F_s \quad (4)$$

$$x_r = G_{rp} F_p + G_{rr} F_r + G_{rs} F_s \quad (5)$$

$$x_s = G_{sp} F_p + G_{sr} F_r + G_{ss} F_s \quad (6)$$

where

G_{qp} is the complex receptance providing the displacement at point q due to a force at point p , etc.

Expressing F_r and F_s in terms of x_r and x_s from Equation (3), and subsequent elimination of x_r and x_s from Equations (4), (5), and (6), gives

$$\frac{x_q}{F_p} = G_{qp} + \frac{k (G_{sp} - G_{rp}) (G_{qr} - G_{qs})}{1 + k(G_{rr} + G_{ss} - G_{rs} - G_{sr})} \quad (7)$$

This may now be rewritten in more general terms as

$$\xi + i\eta = (e + if) + \frac{k(a + ib)}{1 + k(c + id)} \quad (8)$$

where

$$\frac{x_q}{F_p} = \xi + i\eta \quad (9)$$

and a , b , c , d , e , and f are all real. The imaginary part of Equation (8) can be rearranged to the equation of a circle, being

$$\left[\xi - \left(e + \frac{b}{2d} \right) \right]^2 + \left[\eta - \left(f - \frac{a}{2d} \right) \right]^2 = \frac{a^2 + b^2}{4d^2} \quad (10)$$

It is important to note here that the radius of the circular response, as well as the complex coordinates of the center of the circle, may be obtained from these original complex

receptance matrix coupling terms of Equation (10). No iterations in k are necessary; in fact, k drops out of the solution when expressed in this form. Furthermore, it is clearly seen that these circular response properties are purely a function of the imaginary terms (i.e., damping).

Several papers have been published (References 2, 3, and 4) to both mathematically and experimentally substantiate this circular response region, and to employ these circular properties as a possible optimization technique for reducing structural vibration. In a more general sense, Balmford⁵ describes the Vincent circle as a method for providing a reduction of vibration in a local area by adjustment of airframe modes such that modal cancellation will take place to reduce the response for one frequency and one loading condition.

STRAIN ENERGY METHOD

Strain energy is an expression for the potential energy of a structural element and is most commonly expressed in matrix form for the static condition as

$$SE = 1/2 (\delta^T K_e \delta) \quad (11)$$

For the dynamic condition, structural elements possessing the highest strain energies in a given mode of vibration have been shown to be the best candidates for modification to reduce overall structural dynamic amplification.⁶ Two approaches are generally considered, as described in the following sections.

Modal Strain Energy Approach

This approach seeks to reduce vibration by detuning a structure natural frequency to a better position with respect to the forcing frequency. Modal strain energy is calculated for each structural element using the mode shape (eigenvector) for the natural frequency to be modified

$$SE = 1/2 (\phi^T K_e \phi) \quad (12)$$

Elements with the highest strain energies indicate the optimal structural elements to change in order to shift the natural frequency away from the forcing frequency, thereby reducing dynamic amplification.

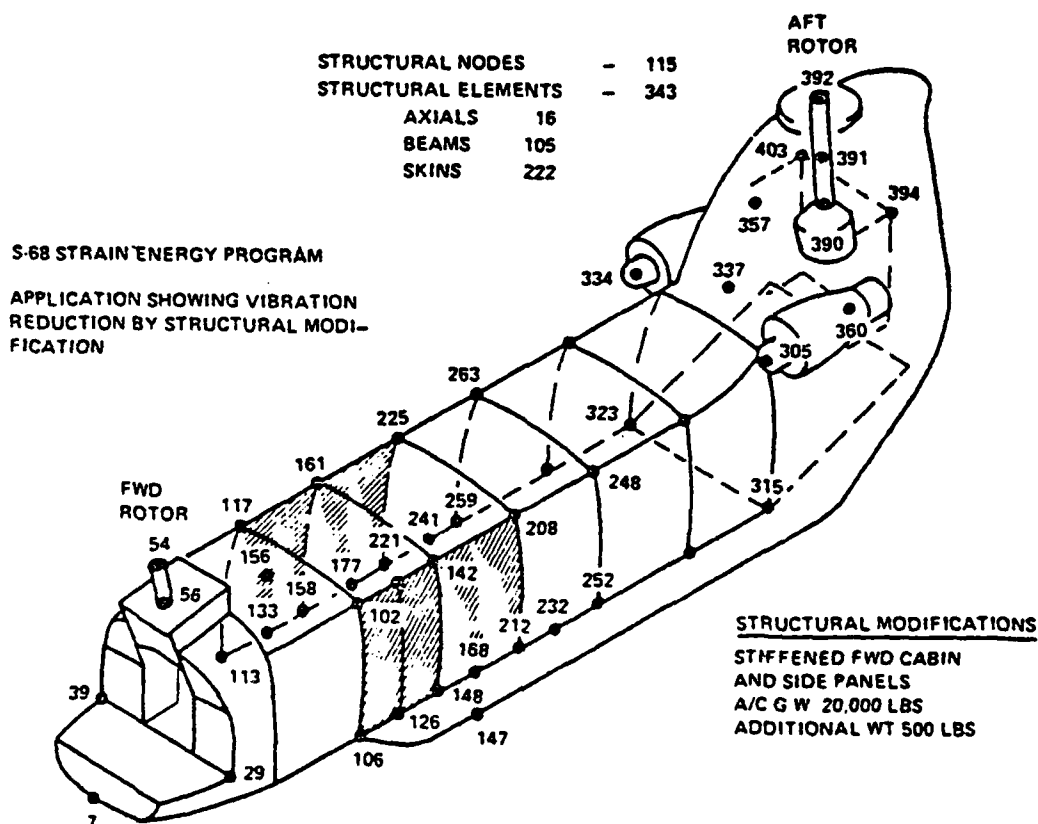
Forced Response Strain Energy Approach

This is an extension of the modal approach that takes into account the response participation of all modes for a particular load application and excitation frequency, including the effects of structural damping and combined forcing function phase relationships. Therefore, the resultant strain energy of each structural element will be a periodic function in time. Sciarra⁶ has done considerable work in this field and has arrived at an expression for the maximum damped forced response element strain energy within the period

$$\begin{aligned} 4(SE)_{\max} = & \delta_R^T K_e \delta_R + \delta_I^T K_e \delta_I \\ & + [(\delta_I^T K_e \delta_I - \delta_R^T K_e \delta_R)^2 \\ & + (\delta_R^T K_e \delta_I + \delta_I^T K_e \delta_R)^2]^{1/2} \end{aligned} \quad (13)$$

Elements with the highest strain energies indicate the elements that are most responsible for the structural dynamic amplification. Because the forced response strain energy approach gives direct information at the specific excitation frequency of interest, it was selected for comparison to the Vincent circle method.

Figure 2 illustrates an application of the strain energy technique. First, the modal strain energy approach was used to selectively stiffen the structure in order to move a fuselage natural frequency to a higher position above the excitation frequency, thereby reducing the dynamic amplification. A damped forced response analysis of the modified structure was then compared to the original structure, and it was confirmed that an overall vibration reduction had resulted in the fuselage area of interest.



Mode	Original Fuselage Hz	Modified Fuselage Hz	Excitation Frequency 11.45 Hz
7	6.687	6.703	Natural Frequency Changed (Mode No. 10, 4th Elastic Mode) - Mode Amplification Factor Down From 9.1 to 5.0
8	7.879	8.160	
9	8.442	8.494	
10	12.03	12.74	
11	12.52	12.79	
12	14.48	14.82	
13	15.69	16.02	
14	16.95	17.22	
15	18.94	19.06	

A damped forced response analysis comparison of the original and the modified fuselage resulted in a vibration reduction for 99 out of 123 degrees-of-freedom.

Figure 2. Boeing-Vertol CH-47A vibration reduction by structural modification (Reference 6).

PROGRAM OBJECTIVES

The purpose of this contracted study was to evaluate the practical applicability of the Vincent circle method, as compared to the forced response strain energy method, for reducing vibration through realistic structural stiffness optimization. The analytical study was performed on the Model AH-1G helicopter, and the effort was limited to application of a single steady-state main rotor 2/rev (10.8 Hz) vertical excitation force with a goal of minimizing the pilot's seat vertical response.

The Vincent circle method was further investigated for usefulness as applied to evaluating mass changes, damping, and ability to optimize dynamic absorber locations.

ANALYTICAL APPROACH

METHOD OF ANALYSIS

For evaluating the Vincent circle method, the receptance matrix technique previously described offers an attractive and direct means to obtain the response circle radius and center-of-location properties based on a single stiffness (or mass) parameter. However, for a feasibility study of this nature, several important disadvantages also exist in that the receptance matrix technique is not easily adapted for evaluation of the following:

- The sensitivity of the circular response region versus element stiffness (or mass) values.
- A coupled stiffness matrix between two points. In dealing with real structure, rarely are we concerned with a single uncoupled parameter like a simple spring, but rather structural elements behaving more like beams that have coupled stiffness matrices. For example, a single variation in the area moment of inertia (I) of a beam affects both the shear translational and rotational degrees-of-freedom between the two ends of the beam.
- Individual element damping variations while the damping for the remainder of the structure remains uniform.
- Tuning sensitivity of a dynamic absorber at different locations on the structure (i.e., effect of backup structure at absorber location).

Since the purpose of this contracted effort was not to evaluate the merits of the receptance matrix technique, and in order to use the same analytical tool for evaluating both the Vincent circle method and the forced response strain energy method, a straightforward linear NASTRAN⁷ analysis was selected for performing the study. Also, due to a unique situation at Bell Helicopter Textron wherein many NASTRAN computer runs can be accomplished quickly and at a low cost, the additional time and cost that would have been required to develop a special purpose receptance matrix manipulation computer program was avoided.

⁷THE NASTRAN USER'S MANUAL, NASA SP-222(03) National Aeronautics and Space Administration, Washington, D. C., July 1976.

As applied to the Vincent circle method, this straightforward NASTRAN approach required the evaluation of several iterations in the particular parameter under investigation to develop the circular response region, from which the response circle radius and center-of-location properties were subsequently determined. However, no restrictions were necessary on what parameters could be selected, and more in-depth information was provided as to the characteristics of the circular response region than if the receptance matrix technique had been employed.

The version of NASTRAN used at the time of this study was Level 16.0.5. This particular level of NASTRAN does support strain energy calculations, but only for static analysis. Although desirable, it was found that the NASTRAN internal modifications necessary to incorporate the complex damped forced response strain energy calculations (Equation 13) were beyond the scope of this study. However, by using the Direct Matrix Abstraction Program (DMAP) capability in NASTRAN, the static strain energy module was incorporated into the dynamics frequency response analysis with the following limitations:

- All applied oscillatory loads must be input at zero degrees phase.
- No damping can be included, thus the applied load and response vector have only real components.

These limitations were required because the statics format of the NASTRAN strain energy module is not compatible for processing complex numbers (i.e., only the real part of a complex number is considered). Therefore, the forced response strain energy expression for a structure element responding to a single resultant applied load with zero damping has now been reduced to

$$SE = 1/2 (\delta_R^T K_e \delta_R) \quad (14)$$

This results in a strain energy distribution that is a close approximation to the strain energy distribution obtained when a small amount of uniform structural damping is included. For the purposes of this study, this undamped strain energy distribution was acceptable for comparison to the Vincent circle results, wherein a small amount of damping must be included as previously explained.

MATHEMATICAL MODELS

Initial stiffness parameter investigations were conducted using a simple elastic-line NASTRAN model of the AH-1G helicopter (Figures 3 and 4). This elastic-line model was originally developed as an AH-1J (Reference 8) and was later modified into the AH-1G configuration (Reference 9). The structural optimization method showing the most potential for reducing vibration through realistic structural stiffness changes was then applied to minimize pilot's seat vertical response using a large complex built-up NASTRAN model of the AH-1G (Figure 5).¹⁰ The elastic-line model was also used to further evaluate the Vincent circle method as applied to mass, damping, and dynamic absorber parameters.

For use in this study, both the elastic-line and the built-up models of References 9 and 10, respectively, were updated to a basic mission-clean wing configuration. To show the similarity of the two models, a comparison of weight data and natural frequency placements is shown in Table 1. From the natural frequency comparisons, in addition to the obvious absence of landing gear skid modes, it is seen that the elastic-line model has no fuselage torsional modes in the zero to thirty hertz frequency range of interest. This is due to inadequate fuselage torsional mass inertia representation in the elastic-line model which, due to the torsional coupling, is also partially responsible for the differences in pylon roll and fuselage lateral bending modes. Note, however, the close agreement between the two models for the pylon pitch and the first and second fuselage vertical bending modes that are of primary importance in this study. Both the elastic-line and built-up models have the same elastic-line representations for the helicopter tailboom structure.

⁸Cronkhite, J. D., and Wilson, W. F., DYNAMIC ANALYSIS OF TWO-PER-REV VIBRATIONS IN THE MODEL AH-1J HELICOPTER - PIP Task No. AH-8-123, Bell Helicopter Textron Report 299-100-021, Fort Worth, Texas, 4 February 1972.

⁹Cronkhite, J. D., XM-97 (20MM) WEAPON ON THE AH-1G - PRELIMINARY DYNAMIC ANALYSIS, Bell Helicopter Textron Inter-office Memo 81:JDC:mb-054, Fort Worth, Texas, 29 May 1973.

¹⁰Cronkhite, J. D., Berry, V. L., and Brunken, J. E., A NASTRAN VIBRATION MODEL OF THE AH-1G HELICOPTER AIRFRAME, U.S. Army Armament Command Report No. R-TR-64-45, Research Directorate, Gen. Thomas J. Rodman Laboratory, Rock Island Arsenal, Rock Island, Illinois, June 1974.

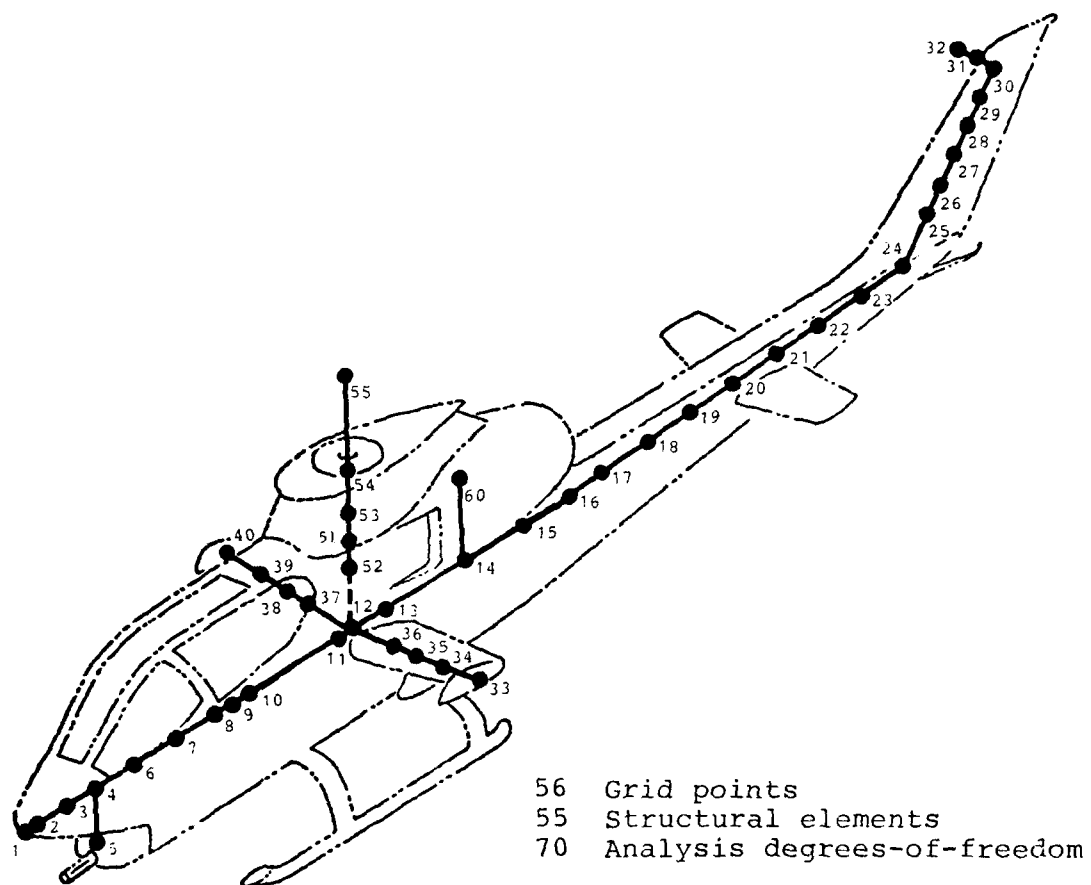


Figure 3. AH-1G elastic-line math model.

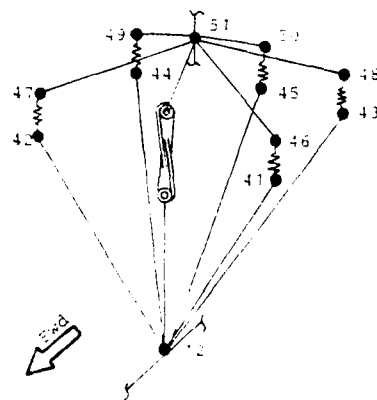
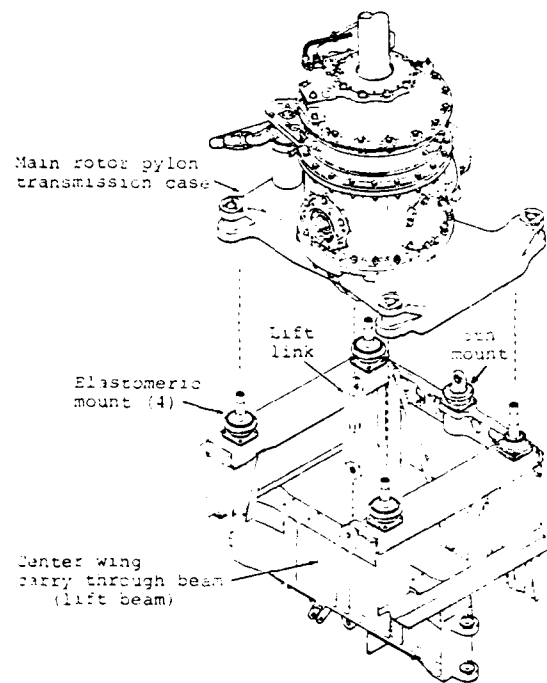


Figure 4. Elastic-line model main rotor pylon.

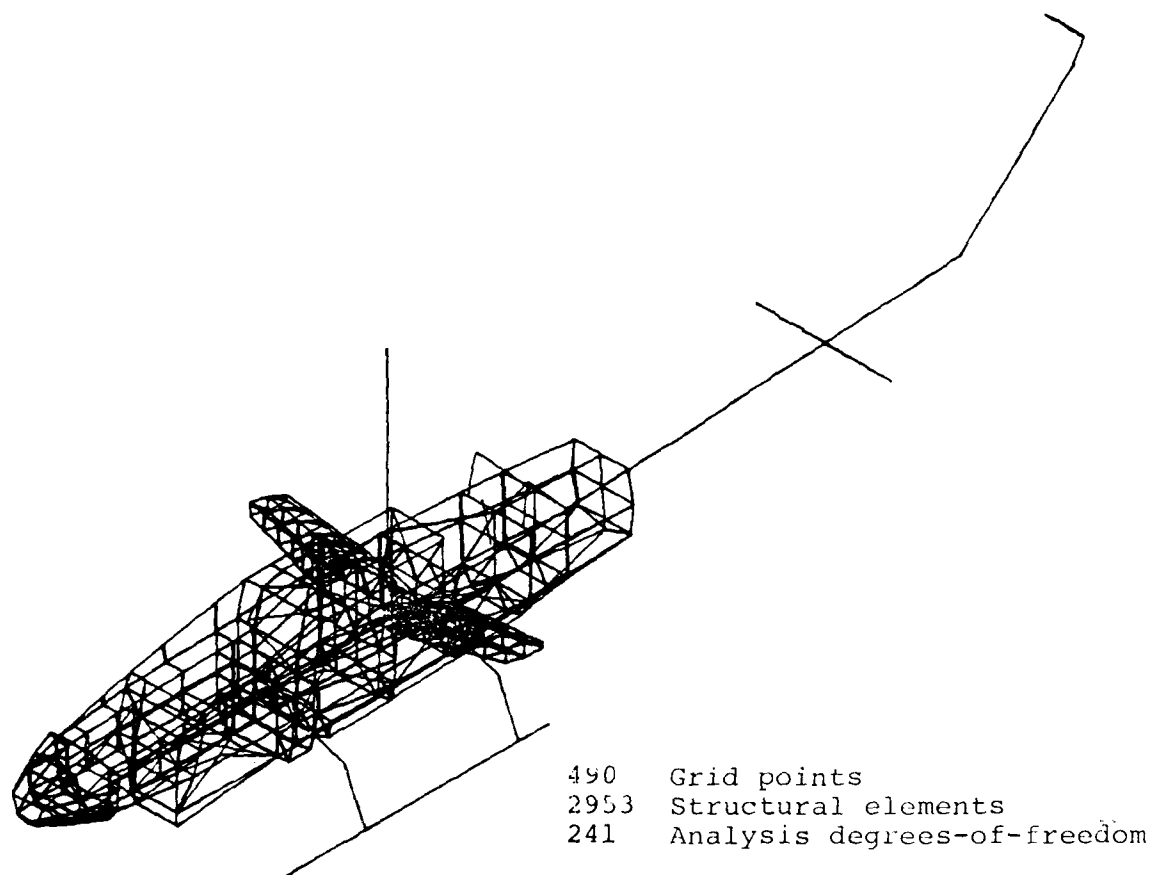


Figure 5. AH-1G built-up math model.

TABLE 1. AH-1G MODEL COMPARISON

Basic Mission-clean Wing	3-D Built-Up Model	Elastic Line Model
Weight Data		
Gross weight (lb)	8394.	8394.
Center-of-gravity { Sta (in.)	192.9	193.1
{ BL (in.)	0.0	0.1
{ WL (in.)	70.6	68.7
Inertias { Roll (lb-in. ²)	1.139×10^7	1.139×10^7
{ Pitch (lb-in. ²)	6.193×10^7	6.200×10^7
{ Yaw (lb-in. ²)	5.196×10^7	5.215×10^7
Natural Frequency Data		
Mode Description	(Hz)	(Hz)
M/R pylon pitch	3.03	3.02
M/R pylon roll	3.90	4.24
1st Fuselage lateral bending	7.14	6.80
1st Fuselage vertical bending	7.94	7.93
1st Skid mode	14.57	-
1st Fuselage torsion	15.66	-
2nd Fuselage lateral bending	17.49	16.70
2nd Fuselage vertical bending	17.49	17.86
2nd Skid mode	18.76	-
3rd Skid mode	19.84	-
2nd Fuselage torsion	21.49	-
4th Skid mode	23.43	-
M/R mast lateral bending	25.28	24.79
M/R mast F/A bending	24.97	25.80
5th Skid mode	25.75	-
3rd Fuselage vertical bending	26.96	29.47
6th Skid mode	29.04	-

The AH-1G elastic-line NASTRAN model (including the DMAP ALTER procedure developed for obtaining undamped forced response element strain energy output) is included as Appendix A.

PRACTICAL CRITERION FOR STRUCTURAL STIFFNESS CHANGES

A practical criterion for stiffness change limitations was developed by considering the classical single degree-of-freedom spring/mass/damper dynamic system that has a resonance dynamic amplification factor of 25 for 2 percent damping. This amplification factor can be reduced to 1.1 by either reducing the stiffness by a factor of 0.5, or by increasing the stiffness by a factor of 10, assuming the mass and damping parameters to remain constant. This 0.5 to 10 stiffness factor range seems to be within the limits of practical considerations even though, realistically speaking, structure designed for strength would not have its stiffness reduced by one-half or increased ten-fold without undergoing a considerable redesign effort (i.e., geometric shape factor, type materials, added weight penalties, etc.)

Based on this practical stiffness change criterion, the forced response strain energy and Vincent circle results were compared to determine which was the most promising method for vibration reduction through realistic structural stiffness optimization.

STIFFNESS PARAMETER INVESTIGATIONS

ELASTIC-LINE MODEL ANALYSIS

The forced response strain energy method was used to determine which structural members had the highest forced response strain energies. Using stiffness parameter variations, these members were then analyzed using the Vincent circle method.

Forced Response Strain Energy Results

Figure 6 is a NASTRAN-generated plot showing a side view of the elastic-line model forced response vertical deformation mode shape. The resultant forced response strain energy distribution is shown in Figure 7. The element identification numbers shown are related to the two-digit GRID numbers at each end of the element, as identified in Figures 3 and 4. The strain energy shown for each element is the total due to the resultant six degrees-of-freedom deflections at each end of the element and the element stiffness matrix as calculated by Equation (14). Since the elastic-line model is essentially symmetric and the applied load at the hub is in the vertical direction, only deflections in the vertical plane are contributing significantly to the strain energy calculation. Note how the strain energy distribution compares to what might be expected from examination of the elastic deformation mode shape of Figure 6.

The elastic-line model NASTRAN forced response strain energy output data are presented in Appendix B.

Vincent Circle Results

As previously shown, this circular response property is based on variations involving single parameters only. However, in this study the Vincent circle method was evaluated with respect to realistic element property changes such as AE axial stiffness and EI bending stiffness parameters, wherever applicable, so that the influence of all stiffness coupling terms would be included.

In all cases, a single 1000-pound 2/rev main rotor vertical excitation force was applied and the vertical response of the pilot's seat was calculated. Unless otherwise stated, all Vincent circle calculations were performed assuming 2-percent uniform structural damping.

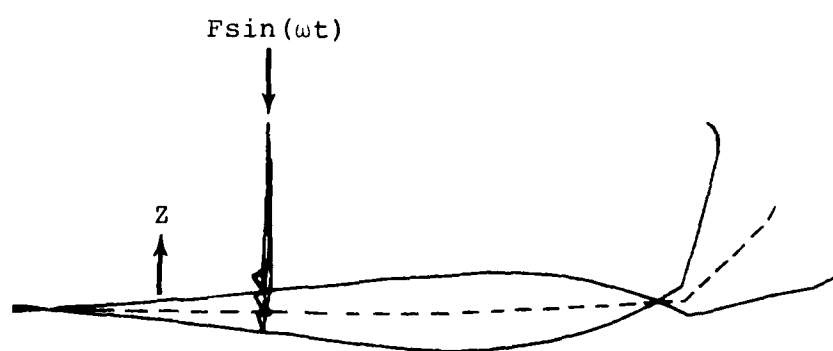


Figure 6. Elastic-line model 2/rev forced response mode shape.

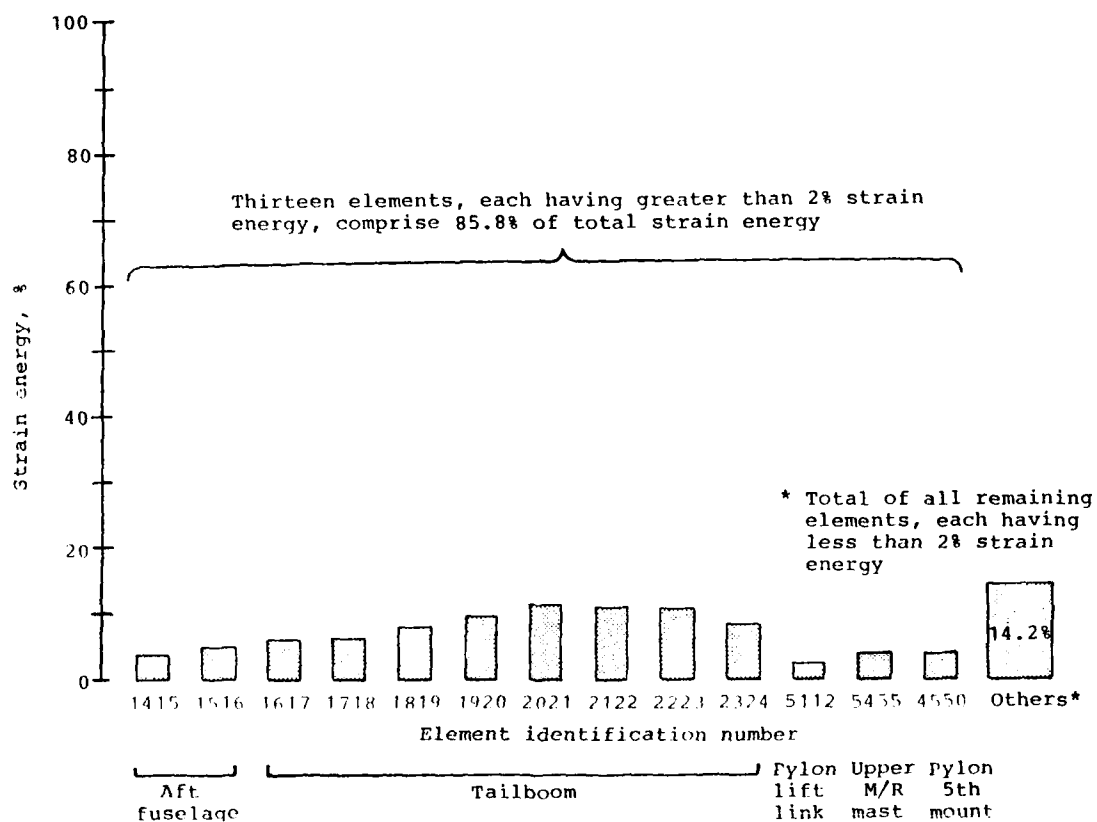


Figure 7. Elastic-line model forced response strain energy distribution.

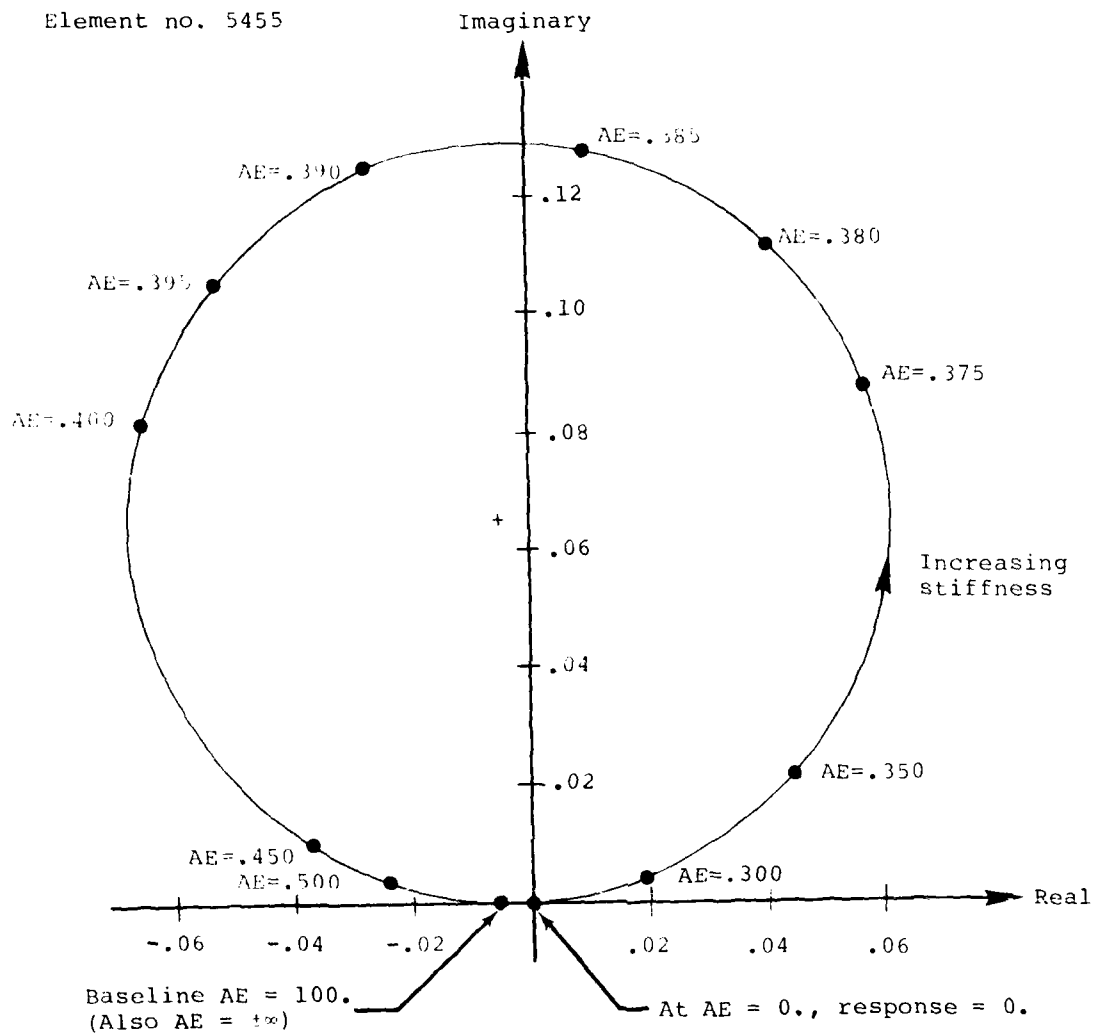
The first application of this method was to verify the circular response property using the elastic-line model. This was accomplished by evaluation of the AE axial stiffness parameter for the upper main rotor mast segment, as shown in Figure 8. Of particular significance are the zero response at zero stiffness and the sensitivity of response to stiffness variations. The zero response at zero stiffness occurs since the main rotor mast provides the only load path. The baseline stiffness value of the element indicates a low initial amplification factor, and the response is seen to be relatively insensitive to stiffness variations except for drastic changes over a very small range of values where, in reality, the element stiffness is the single parameter responsible for the resonance condition. Since the applied load was directed straight down the mast axis, only the mast AE stiffness parameter was evaluated.

With the circular response property thus verified, the remainder of the thirteen elements showing significant forced response strain energies were evaluated for Vincent circle properties of circle diameter and center location. In each case, all parameters were maintained at their original baseline values except for the particular stiffness parameter under investigation. Aft fuselage and tailboom elements were evaluated separately for both AE and vertical EI stiffness parameter variations. It was found that element AE parameter changes produced a response circle which included the baseline AE stiffness response point, as previously shown for element 5455 in Figure 8. Changes in the element EI parameter were found to produce another response circle, but one that was offset from the baseline EI stiffness response point. Further investigations showed that this offset of the EI response circle was due to the I associated stiffness coupling between beam transverse deflection and beam bending (slope change) degrees-of-freedom. This stiffness coupling offset effect was found to be most pronounced for element 1415 (Figure 9). The pylon lift link, element 5112, and the pylon 5th mount, element 4550, are analogous to axially loaded pin-ended rods so that only AE stiffness parameters were evaluated.

The response circle diameter indicates the maximum response change possible due to a particular element stiffness parameter. A normalized circle diameter distribution is shown in Figure 10. Figure 11 shows the maximum reduction in response due to each element stiffness parameter as determined from its circle diameter and center location. In the case of elements evaluated for both AE and EI stiffness parameters, the parameter providing the maximum reduction in response was selected. Note that the trend of element effectiveness established in Figure 10 is similar to that depicted in Figure 11.

Simple elastic line model with 2% uniform structural damping

Element no. 5455



pilot's seat response, inches

Figure 8. Vincent circle plot for upper main rotor mast segment.

Simple elastic line model with 2% uniform structural damping

Element no. 1415

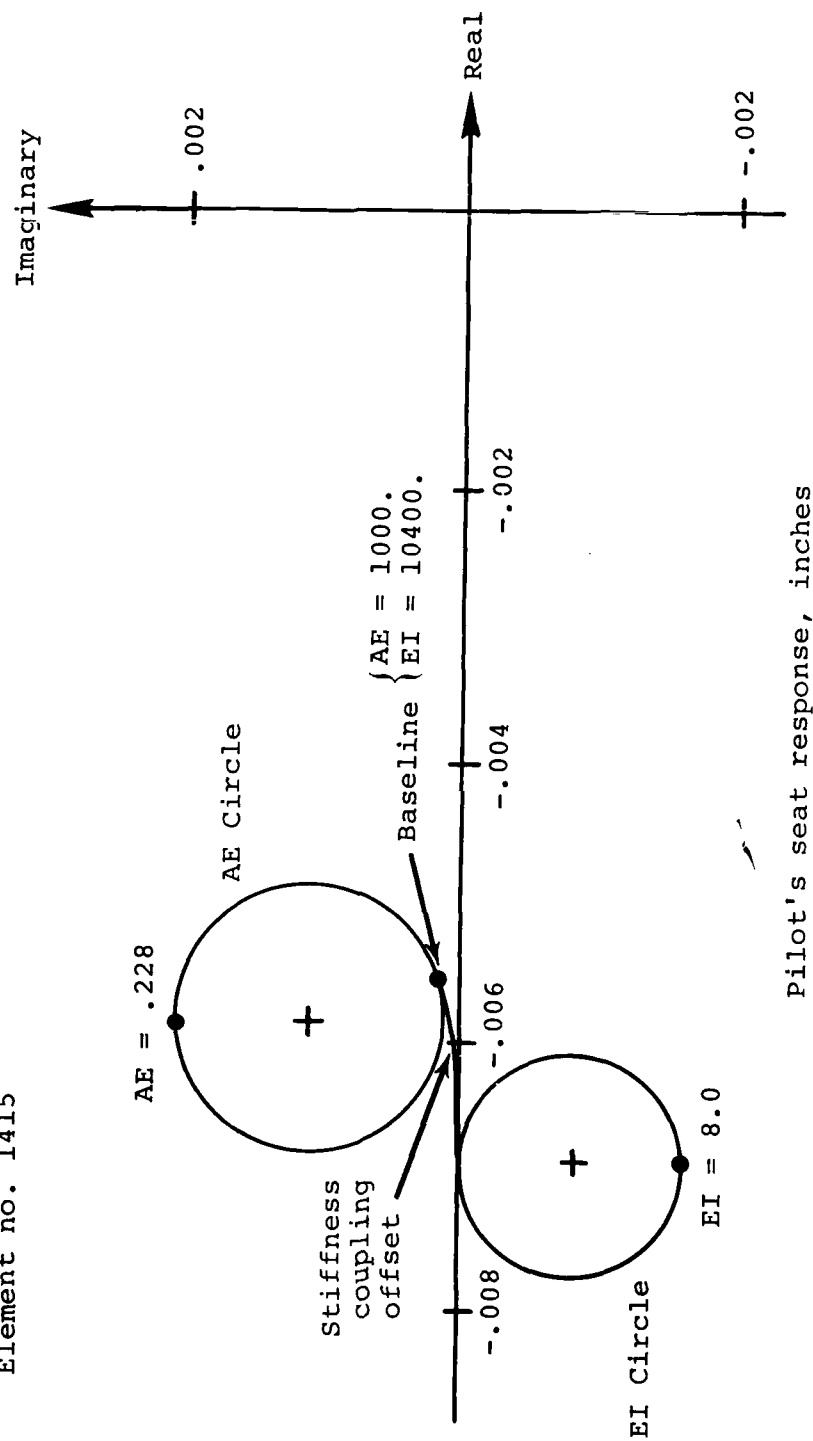


Figure 9. Vincent circle plots for aft fuselage segment.

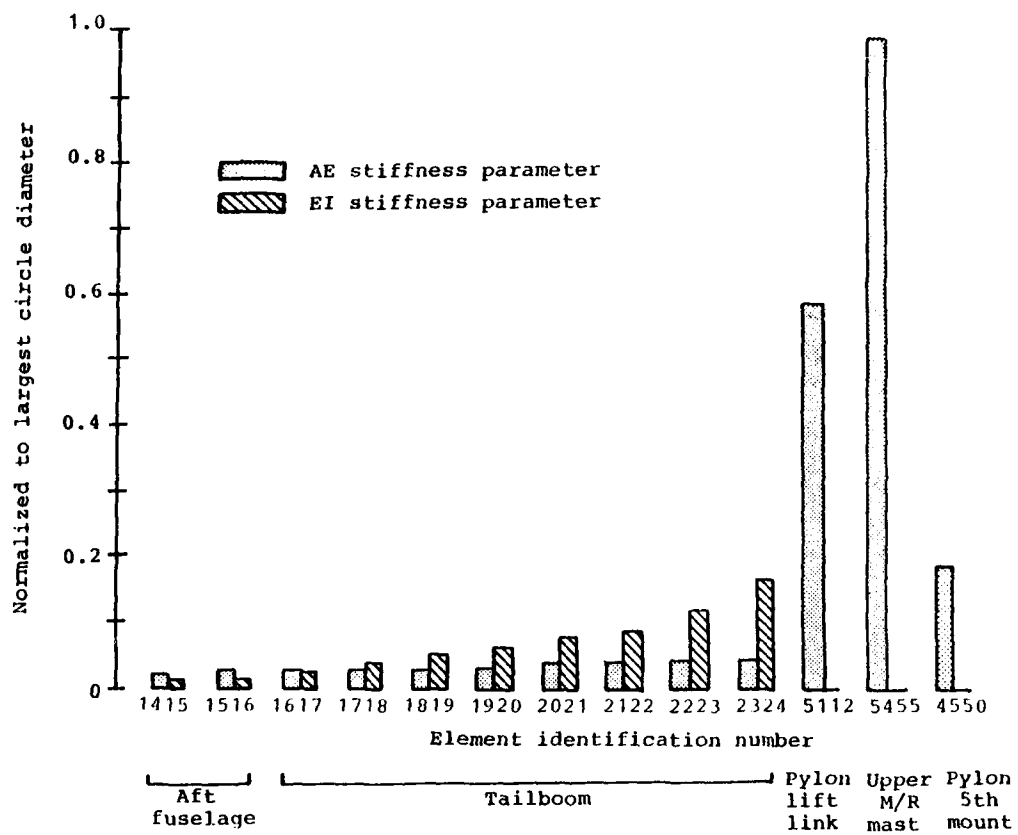


Figure 10. Elastic-line model Vincent circle diameter distribution for pilot's seat response.

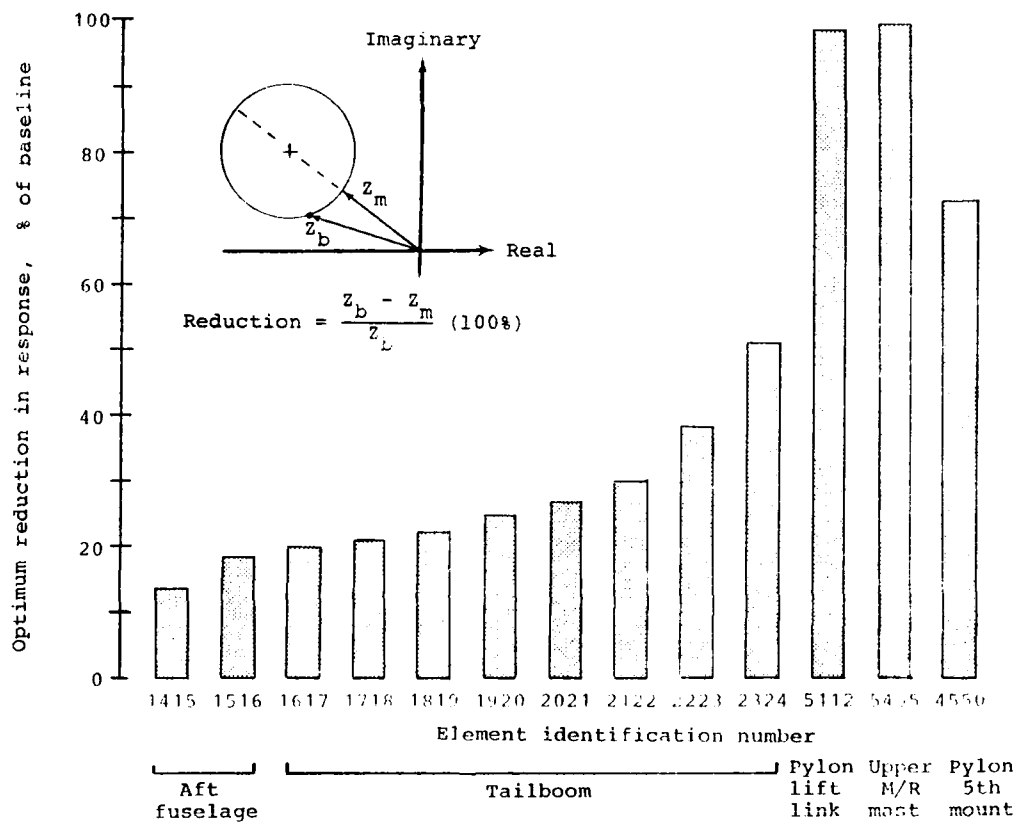


Figure 11. Elastic-line model optimum pilot's seat vibration reduction based on Vincent circle properties.

In other words, in this application the elements with the largest response circle diameters are also capable of achieving the minimum response; however, this is not to be construed as true in all cases.

The most important result to be pointed out is that the Vincent circle properties of circle diameter and center-of-location in the complex plane clearly can be used to determine the minimum response attainable for a particular stiffness parameter; however, no information is provided as to what stiffness value is required to achieve this minimum response. Table 2 shows the drastic and unrealistic stiffness values that were required to produce both the minimum and the maximum pilot's seat vertical response points on the response circle defined by each element stiffness parameter. The two cases where negative stiffnesses are indicated occurred because several elements provided parallel load paths so that a negative stiffness in one element was required to sufficiently reduce the combined elements positive stiffness resultant. In most cases, there is very little difference between the element stiffness values at minimum response and at maximum response (with exceptions for elements 1415, 1516, and 1617 due to their EI response circle offsets (see Figure 9)). Figure 12 further illustrates the stiffness nonlinearity around the response circle by depicting the typical stiffnesses generally found to describe the majority of the circular response region. This inherent property can be somewhat rationalized by considering a single degree-of-freedom model where the dynamic amplification is greatest for the resonance condition and decreases rapidly as the natural frequency is shifted either higher or lower than the excitation frequency.

Strain Energy/Vincent Circle Comparison

Figure 13 compares the undamped forced response strain energy distribution to the 2-percent damped Vincent circle diameter distribution for the same elements of the elastic-line model. Here again, where multiple stiffness parameters were evaluated for the same element, the stiffness parameter producing the largest circle diameter was chosen. It is seen that the Vincent circle method does not give the same distribution picture as the forced response strain energy method. The forced response strain energy method points to the tailboom as the area most responsible for dynamic amplification due to elastic deformation, while the Vincent

TABLE 2. ELASTIC-LINE MODEL ELEMENT STIFFNESS VALUES
FOR MINIMUM AND MAXIMUM PILOT'S SEAT RESPONSE

Element No.	Stiffness Parameter Type	% of Baseline Stiffness	
		Minimum Response	Maximum Response
1415	AE	.021%	.024%
	EI	100%	.071%
1516	AE	.011%	.013%
	EI	100%	.027%
1617	AE	.190%	.213%
	EI	100%	.015%
1718	AE	.181%	.206%
	EI	.020%	.021%
1819	AE	.190%	.210%
	EI	.024%	.028%
1920	AE	.168%	.188%
	EI	.027%	.031%
2021	AE	.152%	.168%
	EI	.035%	.041%
2122	AE	.123%	.139%
	EI	.036%	.043%
2223	AE	.115%	.132%
	EI	.056%	.071%
2324	AE	.104%	.118%
	EI	.109%	.190%
5112	AE	-.775%	-.570%
5455	AE	0%	.387%
4550	AE	-167%	-147%

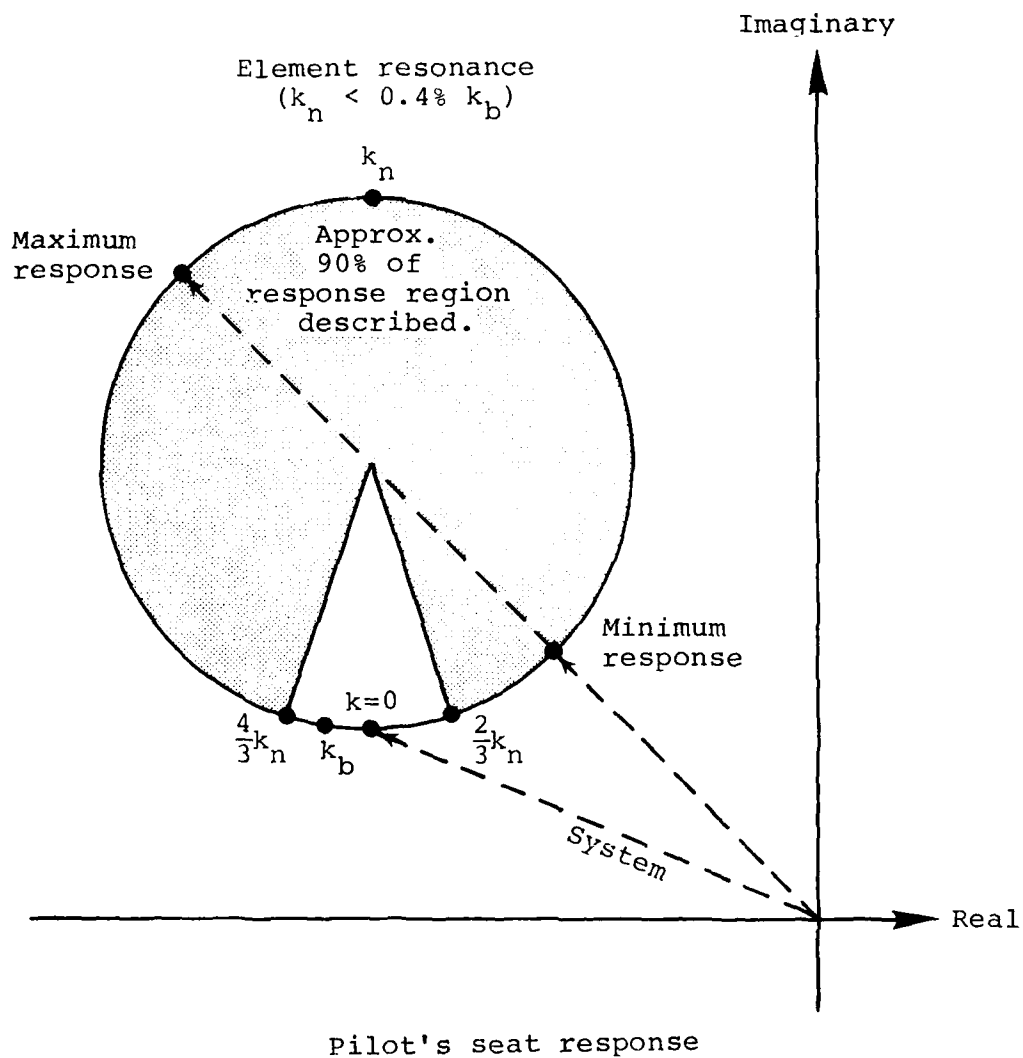


Figure 12. Typical sensitivity of Vincent circle response region.

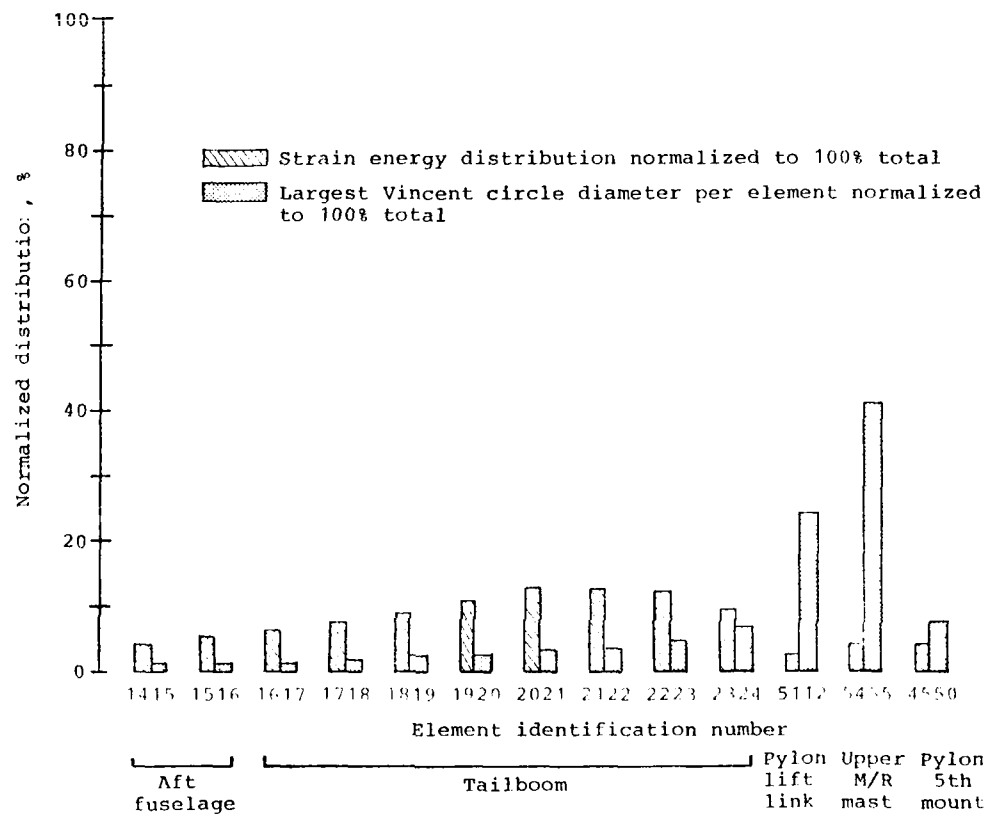


Figure 13. Forced response strain energy comparison to Vincent circle.

circle method points to the pylon as the area having the most potential for reducing vibration at the pilot's seat.

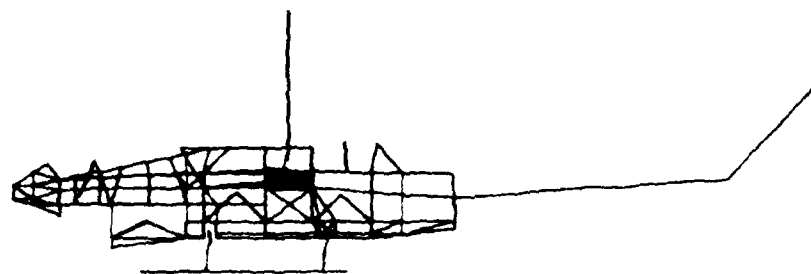
The pylon elements indicated by the Vincent circle method to have the greatest potential for reducing vibration were further evaluated. It was found, as might be strongly suspected from the previous discussion of results, that stiffness variations for these pylon elements within the established confines of the 0.5 to 10 stiffness factor range, even if done collectively, yielded virtually no substantial change in response at the pilot's seat. However, stiffness changes of this same magnitude applied to those tailboom elements initially undergoing substantial elastic deformation, as indicated by the forced response strain energy method, were found to produce significant changes in response at the pilot's seat. Therefore, the forced response strain energy method was determined to be better adapted for vibration reduction through structural stiffness optimization by indicating which structural elements are responsible for the initial dynamic amplification; it was also determined that realistic structural stiffness changes in these elements can efficiently alter the vibration characteristics of the structure.

BUILT-UP MODEL VIBRATION OPTIMIZATION

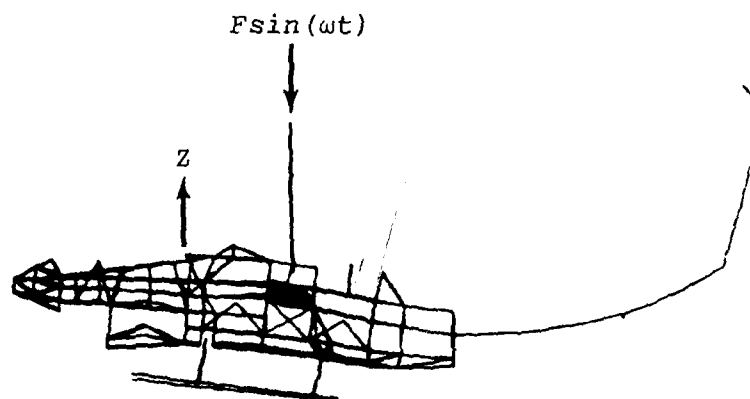
At this point in the investigations, the selected forced response strain energy method was applied to a large complex built-up NASTRAN model (Figure 5).

A NASTRAN-generated plot of a side view of the built-up model forced response vertical deformation mode shape is shown in Figure 14. The resultant undamped forced response strain energy distribution as compared to the distribution for the elastic-line model is shown in Figure 15. The elastic-line model element identification numbers were retained on the figure for reference. Note the similarity of the two distributions. In the case of the aft fuselage and main rotor mast elements, the single element representation of the elastic-line model has been replaced in the built-up model by more detailed modeling involving many elements more uniformly sharing the load, and each accounts for a smaller percentage of the total strain energy.

Previous analyses⁶ have verified that the most dynamically efficient structure for a given mode of vibration is one with a uniform energy distribution. Therefore, the most efficient structural stiffness modifications incorporated for pilot's seat vibration reduction should also result in a more uniform strain energy distribution.



Undeformed shape



Deformed shape

Figure 14. Built-up model 2/rev forced response mode shape.

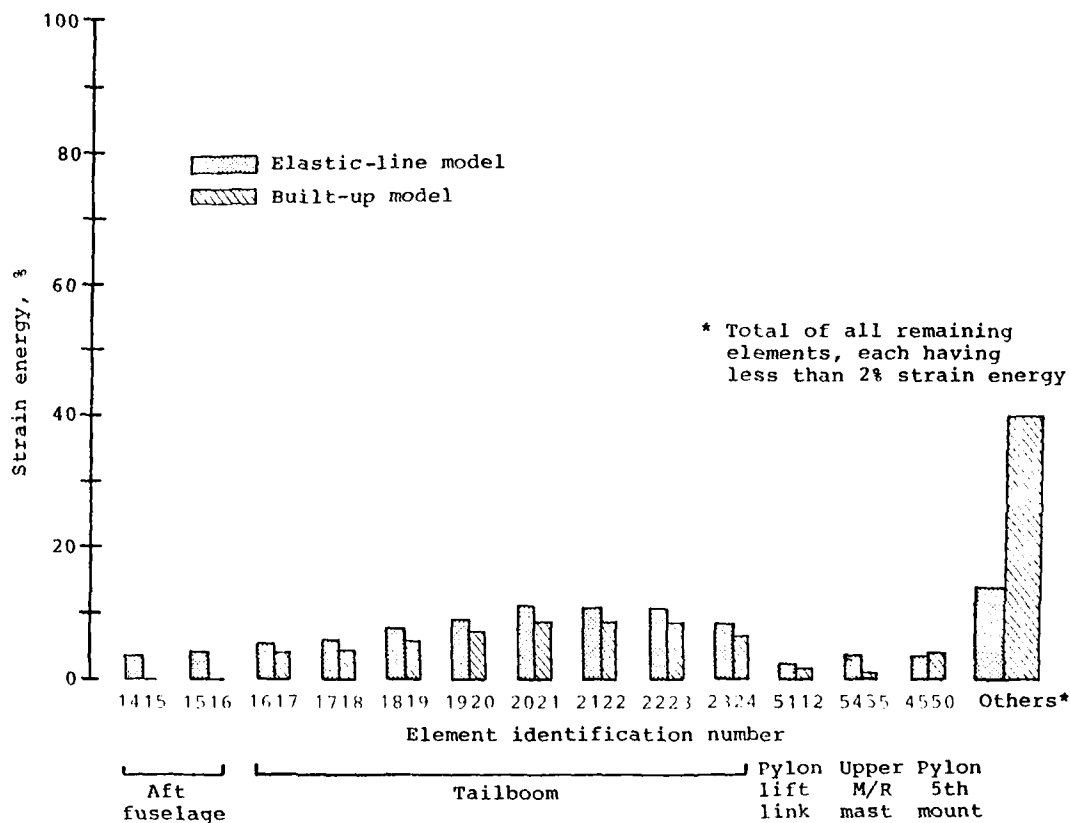


Figure 15. Comparison of forced response strain energy distributions.

From the baseline forced response strain energy distribution, the tailboom elements are seen to possess the most strain energy and were selected as the best candidates for stiffness modifications. The first step was to evaluate both extremes of the selected practical stiffness criterion range. For the stiffer case, the tailboom element with the most strain energy was made ten times stiffer, and the other tailboom elements were made stiffer according to their baseline strain energy ratio. For the softer case, the tailboom element with the least strain energy was made one-half as stiff, and the other tailboom elements were reduced in stiffness according to their baseline strain energy ratio (an additional criterion had to be imposed here - the resultant element stiffness could not be increased because of this strain energy ratio scheme used). The strain energy ratio scheme is shown in further detail in Table 3, along with the accompanying results. In both of these cases the resultant strain energies are more uniformly distributed. In both cases, the pilot's seat response increased in magnitude, but for the stiffer case the response changed phase. This result indicates that a proper stiffness increase, being within the selected practical stiffness criterion range, would result in an absolute zero response at the pilot's seat. Two additional stiffness iterations were required to achieve the desired results. In each case the selected stiffness ratio was applied to tailboom element number 4014220 (largest baseline strain energy) and the other tailboom elements were made stiffer according to their baseline strain energy ratio. As shown in Table 3, it was found that a maximum stiffness increase of 375 percent resulted in near zero response at the pilot's seat and reduced the total strain energy in the tailboom by 46 percent. This also resulted in a slight increase in the strain energies of the two tailboom elements nearest the fuselage. Additional selective stiffening of the tailboom could, no doubt, produce the same zero response results with a more uniform strain energy distribution; however, as it was not the purpose of this study to develop a general optimization procedure, further investigations in this area were not pursued.

A better interpretation of these results may be gained from examination of the simplified forced response mode shapes shown in Figure 16. Here it can easily be seen how the deformed mode shape was altered through the stiffness modifications to place the pilot's seat at a node point.

Although in the foregoing analysis it was possible to achieve zero dynamic response at a particular point under a unique set of circumstances, in no way should these results be interpreted as implying that zero response is always attainable

TABLE 3. BUILT-UP MODEL PILOT'S SEAT VIBRATION REDUCTION

Tailboom Element Identification Number	Baseline		Maximum (SE) _j Made 10X Stiffer		Minimum (SE) _j Made 0.5X Stiffer		Optimized For Minimum Response	
	Unitized Stiffness Ratio	Strain Energy (SE) _j (%)	Stiffness Ratio Applied S _j	Resulting Strain Energy (%)	Stiffness Ratio Applied S _j	Resulting Strain Energy (%)	Stiffness Ratio Applied S _j	Resulting Strain Energy (%)
Elastic Line Model (Ref)								
(1617)	1.0	4.06	4.72	2.59	0.63	3.69	2.24	5.50
(1718)	1.0	4.50	5.23	2.11	0.70	4.00	2.49	4.61
(1819)	1.0	5.72	6.65	1.71	0.89	4.31	3.16	3.84
(1920)	1.0	7.10	8.26	1.41	1.0	5.03	3.92	3.27
(2021)	1.0	8.49	9.87	1.20	1.0	6.31	4.69	2.85
(2122)	1.0	8.60	10.0	1.02	1.0	6.68	4.75	2.50
(2223)	1.0	8.36	9.72	0.91	1.0	6.75	4.62	2.23
(4434520)	1.0	3.23	3.76	0.80	0.50	5.36	1.78	2.04
(2324)	1.0	3.31	3.85	0.72	0.51	5.48	1.83	1.88
Totals =		53.37		12.47		47.61		28.77
1st Fus. vert. mode	7.94 hz		10.58 hz		7.49 hz		9.94 hz	
Pilot's seat response	-.005508 in		.022153 in		-.005874 in		-.000003 in	

$$S_j = \frac{(SE)_j}{8.60} (10.) \quad S_j = \frac{(SE)_j}{3.23} (0.5) \quad S_j = \frac{(SE)_j}{8.60} (4.75)$$

$$\{S_j = 1.0\}$$

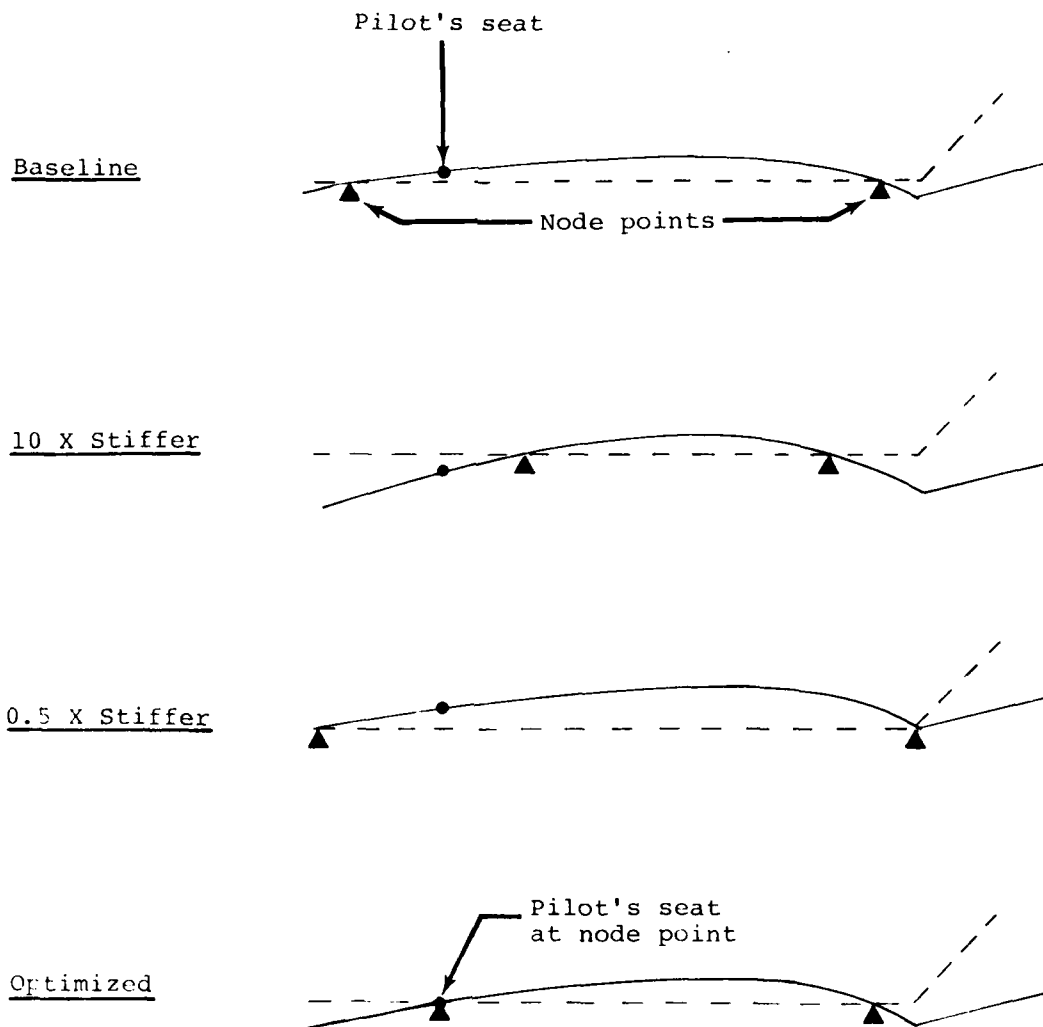


Figure 16. Simplified built-up model forced response mode shapes showing vibration optimization process.

through any type of structural modification. As previously explained in the introduction, many factors need to be considered. Also, for the purposes of this study, no change in mass was considered for any of the stiffness changes evaluated. One of the next most logical steps necessary for any realistic vibration optimization program would be to evaluate the combined effects of both stiffness and the associated weight change. The end product is, of course, a minimum vibration environment obtained through optimization of a structure within a given set of practical criteria.

FURTHER EVALUATION OF THE VINCENT CIRCLE

The Vincent circle phenomenon was further evaluated for mass tuning, damping, and dynamic absorber parameters using the elastic-line model and a simple add-on single degree-of-freedom spring-mass-damper system.

MASS PARAMETER RESULTS

Element mass parameter changes were found to describe the same circle that stiffness changes produce, only the increasing mass traced out the circle in the opposite direction. Data points on the example shown in Figure 17 have been somewhat exaggerated for clarity.

DAMPING PARAMETER RESULTS

Damping is usually not considered as a practical method of effectively altering airframe structural vibration. As shown in Figure 18, both the maximum amplification and the potential of the element for vibration control are greatly reduced by small increases in element damping.

DYNAMIC ABSORBER PARAMETER RESULTS

The adopted procedure for investigating dynamic absorber parameters was to evaluate the effectiveness of one absorber for attenuating 2/rev vertical vibration at the pilot's seat when placed at different locations on the structure; and then, to compare these results to the maximum reductions in pilot's seat response obtained from element stiffness Vincent circle properties at these same locations (as described in Figure 11). The adopted approach does not imply that any such relation between Vincent circle predictions and optimum dynamic absorber locations exists, or has been reported to exist.

The dynamic absorber energy absorption potential was kept constant by maintaining a 25-pound absorber mass and a 0.2% absorber damping coefficient. This required several absorber spring stiffness iterations to achieve the proper tuning of the dynamic absorber at each location due to the different boundary conditions (i.e., backup structure stiffness) which exists throughout the structure. In each case the dynamic absorber was positioned in the vertical direction for reducing pilot's seat vertical vibration. For this study seven dynamic absorber locations were evaluated and the results are shown in Figure 19 as compared to the maximum response reduction distribution obtained from the element stiffness Vincent circle properties.

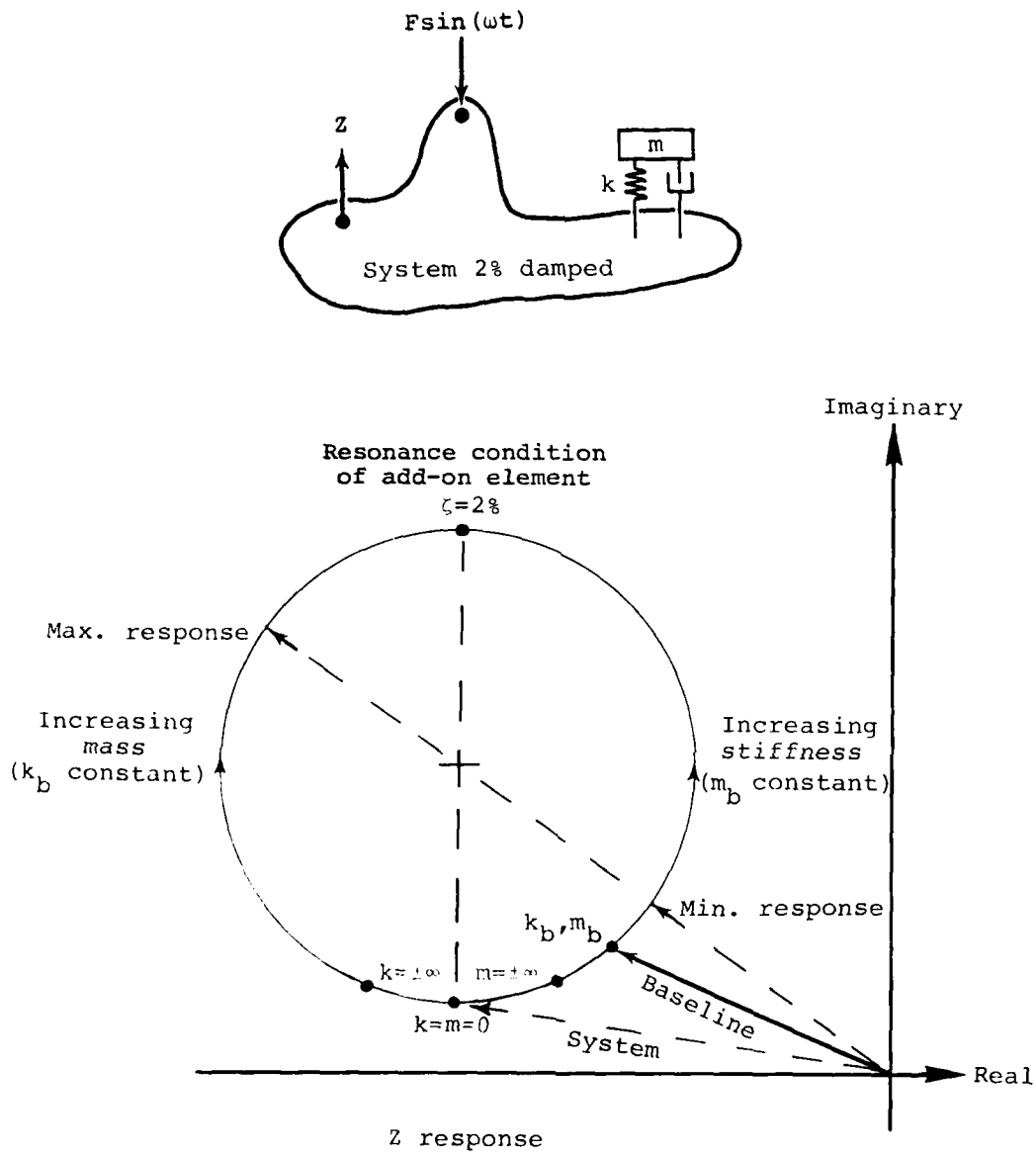


Figure 17. Typical Vincent circle stiffness/mass response region relationships.

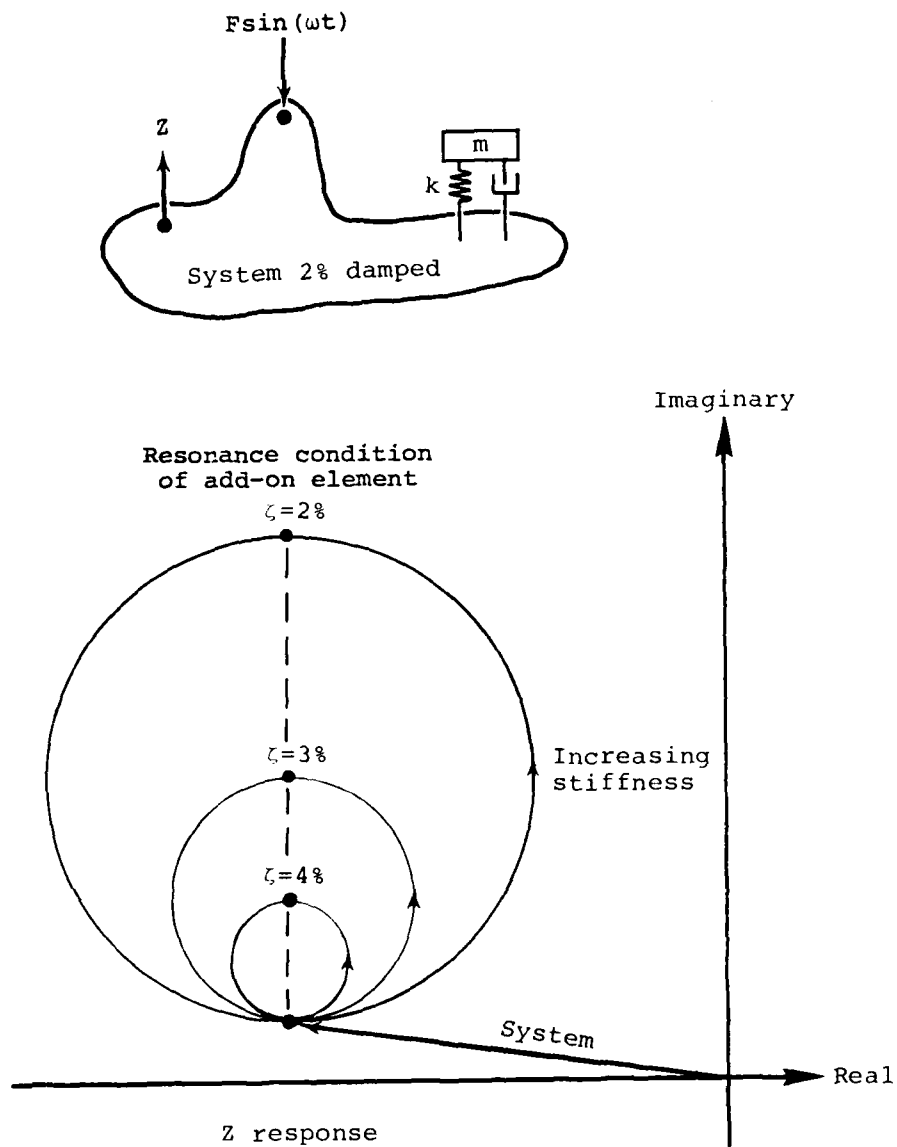


Figure 18. Effect of damping on typical Vincent circle response region.

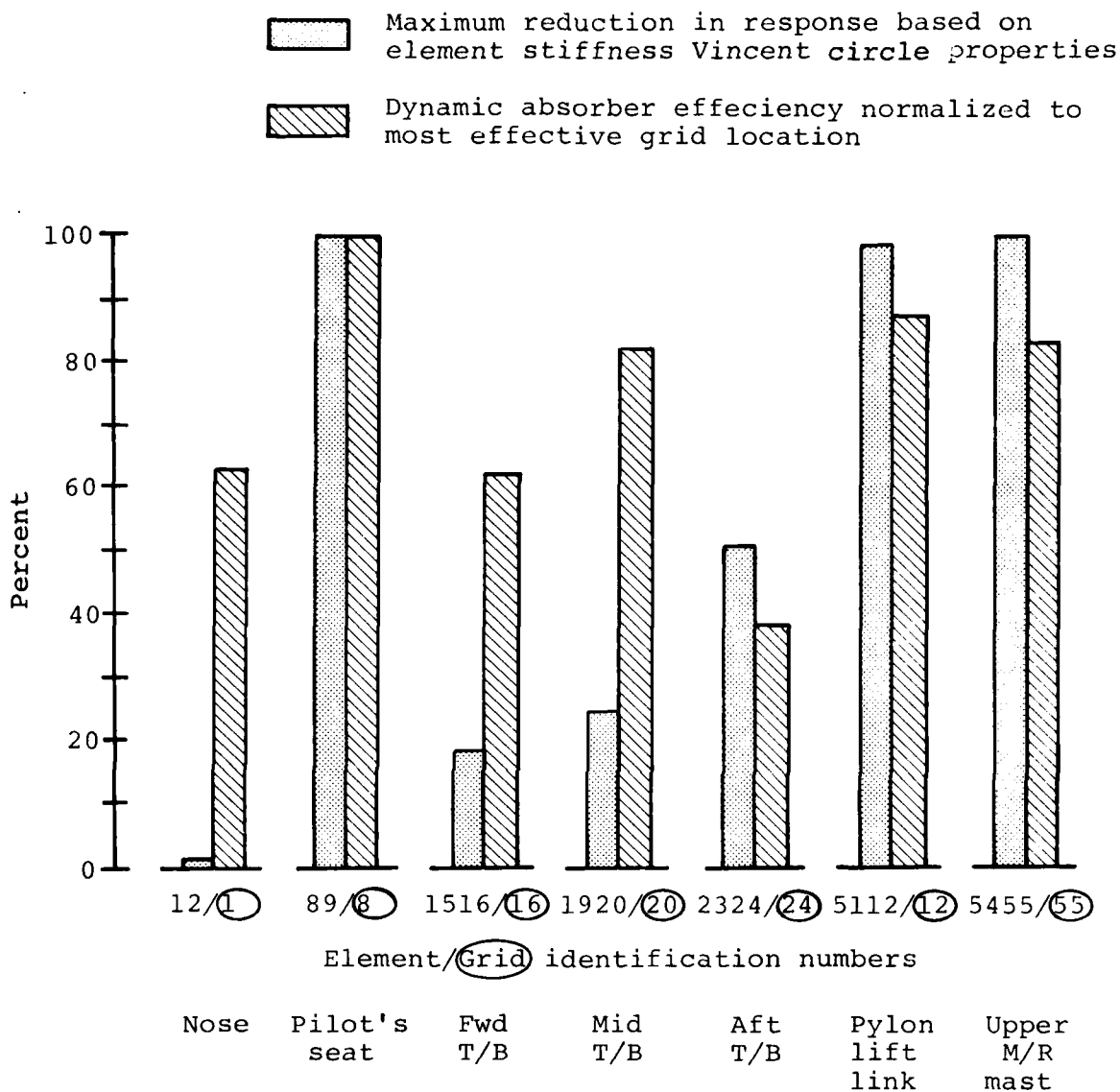


Figure 19. Comparison of Vincent circle properties to dynamic absorber location effectiveness for reducing pilot's seat vibration.

Examination of the dynamic absorber location effectiveness shows that the most efficient location for reducing pilot's seat vibration is at the pilot's seat; but, it also shows that a remote absorber located either at the top of the main rotor mast (grid 55), at the pylon lift link (grid 12), or at the middle of the tailboom (grid 20), would also be significantly effective for reducing vibration at the pilot's seat.

Use of the Vincent circle properties shows that both elements 89 and 5455 are capable of reducing the pilot's seat vibration by 100%. However, these results are inconclusive because any element providing the only load path is ultimately capable of reducing the pilot's seat response to zero if its stiffness is reduced to zero. Further examination of the comparisons shown in Figure 19 shows no definite trends to indicate that the Vincent circle method can be applied to predict optimum dynamic absorber locations.

CONCLUSIONS

The Vincent circle property of a circular response region has been examined and verified by straightforward linear analysis. This property would certainly be of value to the dynamicist for evaluation of a localized portion of structure known to be in, or very near, resonance and which could be controlled by changes involving only a few parameters.

However, for vibration reduction through optimization of an airframe structure where many elements are involved, the forced response strain energy method was found to be more suitable than the Vincent circle method by indicating which structural elements are most responsible for the elastic dynamic amplification. Practical parameter modifications of these elements will most significantly alter the airframe structural dynamic characteristics to reduce vibration. For the more detailed analysis involving complex applied loads, phasing, and damping, the damped forced response strain energy method has the potential benefit of rapid evaluation and optimization of structural vibratory response, which would be particularly beneficial in the predesign stages of an aircraft.

REFERENCES

1. Vincent, A. H., A NOTE ON THE PROPERTIES OF THE VARIATION OF STRUCTURAL RESPONSE WITH RESPECT TO A SINGLE STRUCTURAL PARAMETER WHEN PLOTTED IN THE COMPLEX PLANE, Westland Helicopters Limited Report GEN/DYN/RES/010R, Yeovil, Somerset, England, September 1973.
2. Done, G. T. S., and Hughes, A. D., THE RESPONSE OF A VIBRATING STRUCTURE AS A FUNCTION OF STRUCTURAL PARAMETERS, Journal of Sound and Vibration, Vol. 38, No. 2, 1975, pp. 255-266.
3. Done, G. T. S., and Hughes, A. D., REDUCING VIBRATION BY STRUCTURAL MODIFICATION, Vertica, Vol. 1, No. 1, 1976, pp. 31-38, (paper presented at the First European Rotorcraft and Powered Lift Aircraft Forum at Southampton, September 22-24, 1975).
4. Done, G. T. S., Hughes, A. D., and Webby, J., THE RESPONSE OF A VIBRATING STRUCTURE AS A FUNCTION OF STRUCTURAL PARAMETERS - APPLICATION AND EXPERIMENT, Journal of Sound and Vibration, Vol. 49, No. 2, 1976, pp. 149-159.
5. Balmford, D. E. H., THE CONTROL OF VIBRATION IN HELICOPTERS, Aeronautical Journal, Vol. 81, No. 794, February 1977, pp. 63-67.
6. Sciarra, J. J., USE OF THE FINITE ELEMENT DAMPED FORCED RESPONSE STRAIN ENERGY DISTRIBUTION FOR VIBRATION REDUCTION, Boeing-Vertol Company Report D210-10819-1, U.S. Army Research Office - Durham, Durham, North Carolina, July 1974.
7. THE NASTRAN USER'S MANUAL, NASA SP-222(03) National Aeronautics and Space Administration, Washington, D. C. July 1976.
8. Cronkhite, J. D., and Wilson, W. F., DYNAMIC ANALYSIS OF TWO-PER-REV VIBRATIONS IN THE MODEL AH-1J HELICOPTER - PIP Task No. AH-8-123, Bell Helicopter Textron Report 299-100-021, Fort Worth, Texas, 4 February 1972.
9. Cronkhite, J. D., XM-97 (20MM) WEAPON ON THE AH-1G - PRELIMINARY DYNAMIC ANALYSIS, Bell Helicopter Textron Inter-office Memo 81:JDC:mb-054, Fort Worth, Texas, 29 May 1973.

10. Cronkhite, J. D., Berry, V. L., and Brunken, J. E., A NASTRAN VIBRATION MODEL OF THE AH-1G HELICOPTER AIR-FRAME, U. S. Army Armament Command Report No. R-TR-64-45, Research Directorate, Gen. Thomas J. Rodman Laboratory, Rock Island Arsenal, Rock Island, Illinois, June 1974.

AH-1G ELASTIC-LINE NASTRAN MODEL

```

HANSON,HHT
APP DISP
SOL 8.0
TIME 10
DIAG B-14.19
$$$$$
$$$$$
$$$$$ NASTRAN LEVEL 16.0.5 / RIGID FORMAT SOLUTION 8 / SERIES N
$$$$$
$$$$$ ALTER PACKAGE FOR UNDAMPED FORCED RESPONSE ELEMENT STRAIN ENERGY
$$$$$
$$$$$ NASTRAN LEVEL 16.0.5 DOES NOT SUPPORT ELEMENT STRAIN ENERGY
$$$$$ CALCULATIONS FOR ANY SOLUTION OTHER THAN RIGID FORMAT SOLUTION 1
$$$$$ (STATICS). THIS ALTER PARTITIONS THE OUTPUT FREQUENCY RESPONSE
$$$$$ DATA BLOCKS TO SIMULATE A STATICS SOLUTION BEFORE PASSING THEM
$$$$$ TO THE STRAIN ENERGY CALCULATION MODULE (GPFDR).
$$$$$
$$$$$ RESTRICTIONS ARE:
$$$$$ 1. ALL APPLIED LOADS MUST BE APPLIED AT ZERO DEGREES PHASE
$$$$$ 2. NO DAMPING
$$$$$
$$$$$
$$$$$ ALTER 220 $
PARAM // C.N,NOP / V.N,MINUS1=-1 $
$$$$$
$$$$$
$$$$$ THE BELOW ALTER PARAMETER BY THE NAME OF (NFRQMI) MUST BE SET BY
$$$$$ THE USER. NFRQMI MUST HAVE A VALUE EQUAL TO THE NUMBER OF
$$$$$ FREQUENCIES COMPUTED MINUS ONE; FOR EXAMPLE, IF THE NUMBER OF
$$$$$ FREQUENCIES EQUALS TO 2, THEN NFRQMI=1. THIS CONTROLS THE NUMBER
$$$$$ OF TIMES THE ELEMENT STRAIN ENERGY LOOP IS EXECUTED.
$$$$$
PARAM // C.N,NOP / V.N,NFRQMI=1 $ <<<-- THIS MUST BE SET BY USER
$$$$$
$$$$$ LABEL ESEDYN $
PARTN UPVC,C.P. / UPVC1.,UPVC2. / C.N,1 $
PARTN QPC,C.P. / QPC1.,QPC2. / C.N,1 $
GPFDR CASECC,UPVC1,KELM,KDICT,ECT,EWE,XIN,GPECT.,QPC1 /
UNRGY1,UGPFB1 / C.N,STATICS $
UFP DNRGY1,UGPFB1... // $
PARTN CP.,RP / ,CP1.. / C.N,1 $
PARTN RP.,CP / ,RP1.. / C.N,1 $
EQUIV UPVC2,UPVC / MINUS1 $
EQUIV QPC2,QPC / MINUS1 $
EQUIV CP1,CP / MINUS1 $
EQUIV RP1,RP / MINUS1 $
HEPT ESEDYN,NFRQMI $
ENDALTER $
$$$$$
$$$$$ CASE CONTROL INPUT REQUIRED
$$$$$ ELEMENT STRAIN ENERGY OUTPUT REQUEST:
$$$$$ OR, ESE=ALL
$$$$$ ESE=N (WHERE N IS A SET NUMBER)
$$$$$
$$$$$ BULK DATA INPUT REQUIRED
$$$$$ DMI WHERE NFRQ IS THE NUMBER OF FREQUENCIES COMPUTED
$$$$$ (NFRQ=NFRQMI+1). TWO DMI MATRICES MUST BE INPUT
$$$$$ AS FOLLOWS:
$$$$$ CP - MUST BE A I-COLUMN BY NFRQ-ROW MATRIX.
$$$$$ THE FIRST ROW=1. ALL OTHER ROWS=1.
$$$$$ RP - MUST BE A I-COLUMN BY NFRQ-ROW MATRIX.
$$$$$ ALL ROWS=1., EXCEPT FOR LAST ROW=0.
$$$$$
$$$$$
$$$$$
TITLE= ELASTIC LINE MODEL OF THE AH-1G HELICOPTER
SUBTITLE= UNDAMPED FORCED RESPONSE STRAIN ENERGY METHOD
LATCH= PILIT SFAT RESPONSE TO 1000 LB Z/PREV VERT HUB STEADY
ECHO=BOTH
FREQ=10
OUTPUT
O D O ( SORT 1,REAL ) =ALL
ESE=ALL
ALOAD=1000
HUGEN BULK

```

PAGE 0002

GR ID	1	39.50	0.0	50.0			
GR ID	2	46.0	0.0	50.0			
GR ID	3	61.25	0.0	50.0			
GR ID	4	75.0	0.0	50.0			
GR ID	5	75.5	0.0	29.0			
GR ID	6	93.0	0.0	50.0			
GR ID	7	113.5	0.0	50.0			
GR ID	8	131.5	0.0	50.0			
GR ID	9	140.0	0.0	50.0			
GR ID	10	148.5	0.0	50.0			
GR ID	11	190.0	0.0	50.0			
GR ID	12	197.0	0.0	50.0			
GR ID	13	213.0	0.0	50.0			
GR ID	14	250.0	0.0	50.0			
GR ID	15	277.0	0.0	50.0			
GR ID	16	299.57	0.0	49.59			
GR ID	17	317.72	0.0	50.72			
GR ID	18	338.61	0.0	52.01			
GR ID	19	359.51	0.0	53.31			
GR ID	20	380.42	0.0	54.61			
GR ID	21	401.33	0.0	55.90			
GR ID	22	422.24	0.0	57.20			
GR ID	23	443.15	0.0	58.50			
GR ID	24	464.10	0.0	59.80			
GR ID	25	480.23	0.0	75.40			
GR ID	26	488.93	0.0	83.82			
GR ID	27	497.77	0.0	92.37			
GR ID	28	506.60	0.0	100.91			
GR ID	29	515.43	0.0	109.46			
GR ID	30	520.67	0.0	118.27			
GR ID	31	520.67	7.20	118.27			
GR ID	32	520.67	14.10	118.27			
GR ID	33	199.858	-60.0	62.246			
GR ID	34	196.575	-42.5	61.226			
GR ID	35	194.230	-30.0	60.498			
GR ID	36	192.202	-19.19	59.868			
GR ID	37	192.202	19.19	59.868			
GR ID	38	194.230	30.0	60.498			
GR ID	39	196.575	42.5	61.226			
GR ID	40	199.858	60.0	62.246			
GR ID	41	189.94	-12.375	77.57			
GR ID	42	189.94	12.375	77.57			
GR ID	43	211.72	-12.375	77.57			
GR ID	44	211.72	12.375	77.57			
GR ID	45	214.50	0.0	77.57			
GR ID	46	189.94	-12.375	77.57			
GR ID	47	189.94	12.375	77.57			
GR ID	48	211.72	-12.375	77.57			
GR ID	49	211.72	12.375	77.57			
GR ID	50	214.50	0.0	77.57			
GR ID	51	200.0	0.0	83.8			
GR ID	52	200.0	0.0	77.2			
GR ID	53	200.0	0.0	98.0			
GR ID	54	200.0	0.0	115.0			
GR ID	55	200.0	0.0	153.0			
GR ID	60	248.0	0.0	86.0			
CHAR	12	1	2	0.0	1.0	0.0	1
CHAR	23	2	3	0.0	1.0	0.0	1
CHAR	34	3	4	0.0	1.0	0.0	1
CHAR	45	4	5	0.0	0.0	0.0	1
CHAR	46	4	6	0.0	1.0	0.0	1
CHAR	67	6	7	0.0	1.0	0.0	1
CHAR	78	7	8	0.0	1.0	0.0	1
CHAR	89	8	9	0.0	1.0	0.0	1
CHAR	910	9	10	0.0	1.0	0.0	1
CHAR	1011	10	11	0.0	1.0	0.0	1
CHAR	1112	11	12	0.0	1.0	0.0	1
CHAR	1213	12	13	0.0	1.0	0.0	1
CHAR	1314	13	14	0.0	1.0	0.0	1
CHAR	1415	14	15	0.0	1.0	0.0	1
CHAR	1516	15	16	0.0	1.0	0.0	1
CHAR	1617	16	17	0.0	1.0	0.0	1
CHAR	1718	17	18	0.0	1.0	0.0	1
CHAR	1819	18	19	0.0	1.0	0.0	1
CHAR	1920	19	20	0.0	1.0	0.0	1
CHAR	2021	20	21	0.0	1.0	0.0	1
CHAR	2122	21	22	0.0	1.0	0.0	1
CHAR	2223	22	23	0.0	1.0	0.0	1
CHAR	2324	23	24	0.0	1.0	0.0	1

20MM GUN

PILOT

T/R HUB

XMUN

M/R HUB
ENGINE

CBAR	2425	2425	24	25	0.0	1.0	0.0	1	
CBAR	2526	2526	25	26	0.0	1.0	0.0	1	
CBAR	2627	2627	26	27	0.0	1.0	0.0	1	
CBAR	2728	2728	27	28	0.0	1.0	0.0	1	
CBAR	2829	2829	28	29	0.0	1.0	0.0	1	
CBAR	2930	2930	29	30	0.0	1.0	0.0	1	+2930
+2930			0.0	0.0	0.0	-1.57	0.0	1	-5.21
CBAR	3031	3031	30	31	1.0	0.0	0.0	1	+3031
+3031	56								
CBAR	3132	3132	31	32	1.0	0.0	0.0	1	
CRIGD2	30310	30	31	13					
CBAR	3334	3334	33	34	1.0	0.0	0.0	1	
CBAR	3435	3435	34	35	1.0	0.0	0.0	1	
CBAR	3536	3536	35	36	1.0	0.0	0.0	1	
CBAR	3612	3612	36	12	1.0	0.0	0.0	1	+3612
+3612			0.0	0.0	0.0	-4.798	0.0	1	9.868
CBAR	1237	1237	12	37	1.0	0.0	0.0	1	
+1237			-4.798	0.0	9.868	0.0	0.0	1	0.0
CBAR	3738	3738	37	38	1.0	0.0	0.0	1	
CBAR	3839	3839	38	39	1.0	0.0	0.0	1	
CBAR	3940	3940	39	40	1.0	0.0	0.0	1	
CRIGD1	1240	12	41	42	43	44	45		
CRIGD1	5140	51	46	47	48	49	50		
CBAR	5112	5112	51	12	0.0	1.0	0.0	1	+LIFTLNK
+LIFTLNK			-3.10	0.0	-7.90	-0.1	0.0	1	16.15
CELAS1	41461	1	41	1	46	1			
CELAS1	41462	2	41	2	46	2			
CELAS1	41463	3	41	3	46	3			
CELAS1	42471	1	42	1	47	1			
CELAS1	42472	2	42	2	47	2			
CELAS1	42473	3	42	3	47	3			
CELAS1	43481	1	43	1	48	1			
CELAS1	43482	2	43	2	48	2			
CELAS1	43483	3	43	3	48	3			
CELAS1	44491	1	44	1	49	1			
CELAS1	44492	2	44	2	49	2			
CELAS1	44493	3	44	3	49	3			
CELAS1	45503	33	45	3	50	3			
CRIGD2	515253	51	52	123456	53	12			
CBAR	5253	5253	52	53	0.0	1.0	0.0	1	+5253
+5253	56								
CBAR	5354	5354	53	54	0.0	1.0	0.0	1	
CBAR	5455	5455	54	55	0.0	1.0	0.0	1	
CRIGD1	1460	14	60						
PBAR	12	1	1000.	1650.	250.	200.			
PBAR	23	1	1000.	3300.	700.	200.			
PBAR	34	1	1000.	5350.	1100.	200.			
PBAR	46	1	1000.	5800.	1100.	225.			
PBAR	67	1	1000.	7300.	2750.	850.			
PBAR	78	1	1000.	7300.	3000.	850.			
PBAR	89	1	1000.	7300.	3200.	850.			
PBAR	910	1	1000.	9750.	8200.	2000.			
PBAR	1011	1	1000.	12750.	14710.	3250.			
PBAR	1112	1	1000.	18000.	14710.	3150.			
PBAR	1213	1	1000.	18000.	14710.	3150.			
PBAR	1314	1	1000.	13900.	11670.	2900.			
PBAR	1415	1	1000.	12100.	10400.	2650.			
PBAR	1516	1	1000.	8850.	9300.	2100.			
PBAR	1617	1	42.7403	5138.39	6244.61	3326.62			
PBAR	1718	1	47.4632	4686.89	6300.05	2387.82			
PBAR	1819	1	41.4892	3376.80	4650.61	1863.98			
PBAR	1920	1	38.7424	2797.46	3323.30	1422.92			
PBAR	2021	1	37.5606	2419.04	2301.92	1113.34			
PBAR	2122	1	36.7154	1919.77	1782.38	881.70			
PBAR	2223	1	34.7744	1418.76	1322.74	634.50			
PBAR	2324	1	35.5467	1008.00	1159.10	428.36			
PBAR	2425	1	38.50	182.6	5150.	113.5			
PBAR	2526	1	35.13	168.0	1900.	81.2			
PBAR	2627	1	32.70	152.0	1620.	69.0			
PBAR	2728	1	30.25	135.0	1540.	56.8			
PBAR	2829	1	27.85	100.0	1060.	48.5			
PBAR	2930	1	25.45	72.0	650.	43.7			
PBAR	3031	1	1000.	5.5	5.5	11.0			
PBAR	3132	1	1000.	3.5	3.5	7.0			
PBAR	3334	1	1000.	2600.	454.	230.			
PBAR	3435	1	1000.	4250.	1041.	380.			
PBAR	3536	1	1000.	8250.	1485.	560.			
PBAR	3612	1	1000.	9912.	1683.	5150.			
PBAR	1237	1	1000.	9912.	1683.	5150.			

```

PBAR 3738 1 1000. 8250. 1485. 560.
PBAR 3839 1 1000. 4250. 1031. 380.
PBAR 3940 1 1000. 2600. 454. 270.
PBAR 5112 1 25.81
PELAS 1 28125.
PELAS 2 28125.
PELAS 3 4500.
PELAS 33 20000.
PBAR 5253 1 100. 72. 72. 144.
PBAR 5354 1 100. 135. 135. 270.
PBAR 5455 1 100. 120. 120. 240.
MAT1 1 1.0+6 1.0+6
CONM2 1 1 12.029
CONM2 2 2 34.965
CONM2 3 3 86.882
CONM2 4 4 198.829
CONM2 5 5 253.4
CONM2 6 6 439.371
CONM2 7 7 561.594
CONM2 8 8 355.019
CONM2 9 9 189.893
CONM2 10 10 714.319
CONM2 11 11 686.484
CONM2 12 12 125.393
*H112 0.849+6
CONM2 13 13 836.348
CONM2 14 14 554.022
CONM2 15 15 296.573
CONM2 16 16 87.781
CONM2 17 17 33.058
CONM2 18 18 43.977
CONM2 19 19 60.541
CONM2 20 20 41.474
CONM2 21 21 48.633
CONM2 22 22 22.713
CONM2 23 23 15.102
CONM2 24 24 44.152
CONM2 25 25 19.136
CONM2 26 26 6.809
CONM2 27 27 11.934
CONM2 28 28 8.475
CONM2 29 29 4.968
CONM2 30 30 2.544
CONM2 300 30 25.994
CONM2 31 31 11.282
CONM2 32 32 34.066
CONM2 33 33 9.489
CONM2 34 34 35.704
CONM2 35 35 36.459
CONM2 36 36 95.577
CONM2 37 37 95.577
CONM2 38 38 36.459
CONM2 39 39 35.704
CONM2 40 40 9.489
CONM2 51 51 103.895
CONM2 52 52 115.708
CONM2 53 53 270.518
CONM2 54 54 125.560
CONM2 55 55 33.249
CONM2 550 55 947.5
CONM2 60 60 585.35
*ENG 17800. 109500. 94700.
PARAM WMASS 0.0259
PARAM GRDPNT 0
FREQ 10 10.8
RLDADZ 1000 55.3 0 99 0
DAHEA 55.3 55 3 1000.
TABLED1 99
*H(F) 0.0 1.0 200.0 1.0 END
*****
$ THESE DMI MATRICES MUST BE INPUT FOR ELEMENT DYNAMIC STRAIN ENERGY
$ CALCULATIONS - CONSULT ALTER PACKAGE IN EXECUTIVE BOOK FOR DETAILS.
DMI CP 0 2 1 1 1
DMI CP 1 1 0. 2 1.
DMI RP 0 2 1 1 1
DMI RP 1 1 1. 2 0.
*****
ENDATA
END*

```

*H112

*ENG

*H(F)

APPENDIX A. 1977-1978

NASTRAN EXPLICIT CONTROL DECK F (CH)

58

ELASTIC LINE MODEL OF THE AH-1G HELICOPTER
UNDAMPED FORCED RESPONSE STRAIN ENERGY METHOD
PILOT SEAT RESPONSE TO 1000 LH 2/REV VERT HUB SHEAR

CASE CUNTRUL DECK ECHU

CARD
COUNT

1 TITLE# ELASTIC LINE MODEL OF THE AH-1G HELICOPTER
2 SUBTITLE# UNDAMPED FORCED RESPONSE STRAIN ENERGY METHOD
3 LAHEL# PILOT SEAT RESPONSE TO 1000 LH 2/REV VERT HUB SHEAR
4 ECHU#GTH
5 FREQ#10
6 OUTPUT
7 DISPS#RT1,HEAL#ALL
8 ES#ALL
9 DLOAD#1000
10 BEGIN RULK

10710101 2/REV VERY HIGH S. A. R.

[illegible]

CLASSIC LINE MODEL OF THE AIR-IG DELICHOPTER
UNDAMPED FORCED RESPONSE STRAIN ENERGY METHOD

PILOT SEAT RESPONSE TO 1000 11 2/REV VERT HUB SHAFT

INPUT	4	5	6	7	8	9	10
1	1718	17	0.0	0.0	0.0	0.0	0.0
CHAR	1819	18	0.0	0.0	0.0	0.0	0.0
CHAR	1920	19	0.0	0.0	0.0	0.0	0.0
CHAR	2021	20	0.0	0.0	0.0	0.0	0.0
CHAR	2122	21	0.0	0.0	0.0	0.0	0.0
CHAR	2223	22	0.0	0.0	0.0	0.0	0.0
CHAR	2324	23	0.0	0.0	0.0	0.0	0.0
CHAR	2425	24	0.0	0.0	0.0	0.0	0.0
CHAR	2526	25	0.0	0.0	0.0	0.0	0.0
CHAR	2627	26	0.0	0.0	0.0	0.0	0.0
CHAR	2728	27	0.0	0.0	0.0	0.0	0.0
CHAR	2829	28	0.0	0.0	0.0	0.0	0.0
CHAR	2930	29	0.0	0.0	0.0	0.0	0.0
CHAR	3031	30	0.0	0.0	0.0	0.0	0.0
CHAR	3132	31	0.0	0.0	0.0	0.0	0.0
CHAR	3233	32	0.0	0.0	0.0	0.0	0.0
CHAR	3334	33	0.0	0.0	0.0	0.0	0.0
CHAR	3435	34	0.0	0.0	0.0	0.0	0.0
CHAR	3536	35	0.0	0.0	0.0	0.0	0.0
CHAR	3637	36	0.0	0.0	0.0	0.0	0.0
CHAR	3738	37	0.0	0.0	0.0	0.0	0.0
CHAR	3839	38	0.0	0.0	0.0	0.0	0.0
CHAR	3940	39	0.0	0.0	0.0	0.0	0.0
CHAR	4041	40	0.0	0.0	0.0	0.0	0.0
CHAR	4142	41	0.0	0.0	0.0	0.0	0.0
CHAR	4243	42	0.0	0.0	0.0	0.0	0.0
CHAR	4344	43	0.0	0.0	0.0	0.0	0.0
CHAR	4445	44	0.0	0.0	0.0	0.0	0.0
CHAR	4546	45	0.0	0.0	0.0	0.0	0.0
CHAR	4647	46	0.0	0.0	0.0	0.0	0.0
CHAR	4748	47	0.0	0.0	0.0	0.0	0.0
CHAR	4849	48	0.0	0.0	0.0	0.0	0.0
CHAR	4950	49	0.0	0.0	0.0	0.0	0.0
CHAR	5051	50	0.0	0.0	0.0	0.0	0.0
CHAR	5152	51	0.0	0.0	0.0	0.0	0.0
CHAR	5253	52	0.0	0.0	0.0	0.0	0.0
CHAR	5354	53	0.0	0.0	0.0	0.0	0.0
CHAR	5455	54	0.0	0.0	0.0	0.0	0.0
CHAR	5556	55	0.0	0.0	0.0	0.0	0.0
CHAR	5657	56	0.0	0.0	0.0	0.0	0.0
CHAR	5758	57	0.0	0.0	0.0	0.0	0.0
CHAR	5859	58	0.0	0.0	0.0	0.0	0.0
CHAR	5960	59	0.0	0.0	0.0	0.0	0.0
CHAR	6061	60	0.0	0.0	0.0	0.0	0.0
CHAR	6162	61	0.0	0.0	0.0	0.0	0.0
CHAR	6263	62	0.0	0.0	0.0	0.0	0.0
CHAR	6364	63	0.0	0.0	0.0	0.0	0.0
CHAR	6465	64	0.0	0.0	0.0	0.0	0.0
CHAR	6566	65	0.0	0.0	0.0	0.0	0.0
CHAR	6667	66	0.0	0.0	0.0	0.0	0.0
CHAR	6768	67	0.0	0.0	0.0	0.0	0.0
CHAR	6869	68	0.0	0.0	0.0	0.0	0.0
CHAR	6970	69	0.0	0.0	0.0	0.0	0.0
CHAR	7071	70	0.0	0.0	0.0	0.0	0.0
CHAR	7172	71	0.0	0.0	0.0	0.0	0.0
CHAR	7273	72	0.0	0.0	0.0	0.0	0.0
CHAR	7374	73	0.0	0.0	0.0	0.0	0.0
CHAR	7475	74	0.0	0.0	0.0	0.0	0.0
CHAR	7576	75	0.0	0.0	0.0	0.0	0.0
CHAR	7677	76	0.0	0.0	0.0	0.0	0.0
CHAR	7778	77	0.0	0.0	0.0	0.0	0.0
CHAR	7879	78	0.0	0.0	0.0	0.0	0.0
CHAR	7980	79	0.0	0.0	0.0	0.0	0.0
CHAR	8081	80	0.0	0.0	0.0	0.0	0.0
CHAR	8182	81	0.0	0.0	0.0	0.0	0.0
CHAR	8283	82	0.0	0.0	0.0	0.0	0.0
CHAR	8384	83	0.0	0.0	0.0	0.0	0.0
CHAR	8485	84	0.0	0.0	0.0	0.0	0.0
CHAR	8586	85	0.0	0.0	0.0	0.0	0.0
CHAR	8687	86	0.0	0.0	0.0	0.0	0.0
CHAR	8788	87	0.0	0.0	0.0	0.0	0.0
CHAR	8889	88	0.0	0.0	0.0	0.0	0.0
CHAR	8990	89	0.0	0.0	0.0	0.0	0.0
CHAR	9091	90	0.0	0.0	0.0	0.0	0.0
CHAR	9192	91	0.0	0.0	0.0	0.0	0.0
CHAR	9293	92	0.0	0.0	0.0	0.0	0.0
CHAR	9394	93	0.0	0.0	0.0	0.0	0.0
CHAR	9495	94	0.0	0.0	0.0	0.0	0.0
CHAR	9596	95	0.0	0.0	0.0	0.0	0.0
CHAR	9697	96	0.0	0.0	0.0	0.0	0.0
CHAR	9798	97	0.0	0.0	0.0	0.0	0.0
CHAR	9899	98	0.0	0.0	0.0	0.0	0.0
CHAR	9900	99	0.0	0.0	0.0	0.0	0.0
CHAR	10001	100	0.0	0.0	0.0	0.0	0.0
CHAR	10102	101	0.0	0.0	0.0	0.0	0.0
CHAR	10203	102	0.0	0.0	0.0	0.0	0.0
CHAR	10304	103	0.0	0.0	0.0	0.0	0.0
CHAR	10405	104	0.0	0.0	0.0	0.0	0.0
CHAR	10506	105	0.0	0.0	0.0	0.0	0.0
CHAR	10607	106	0.0	0.0	0.0	0.0	0.0
CHAR	10708	107	0.0	0.0	0.0	0.0	0.0
CHAR	10809	108	0.0	0.0	0.0	0.0	0.0
CHAR	10910	109	0.0	0.0	0.0	0.0	0.0
CHAR	11011	110	0.0	0.0	0.0	0.0	0.0
CHAR	11112	111	0.0	0.0	0.0	0.0	0.0
CHAR	11213	112	0.0	0.0	0.0	0.0	0.0
CHAR	11314	113	0.0	0.0	0.0	0.0	0.0
CHAR	11415	114	0.0	0.0	0.0	0.0	0.0
CHAR	11516	115	0.0	0.0	0.0	0.0	0.0
CHAR	11617	116	0.0	0.0	0.0	0.0	0.0
CHAR	11718	117	0.0	0.0	0.0	0.0	0.0
CHAR	11819	118	0.0	0.0	0.0	0.0	0.0
CHAR	11920	119	0.0	0.0	0.0	0.0	0.0
CHAR	12021	120	0.0	0.0	0.0	0.0	0.0
CHAR	12122	121	0.0	0.0	0.0	0.0	0.0
CHAR	12223	122	0.0	0.0	0.0	0.0	0.0
CHAR	12324	123	0.0	0.0	0.0	0.0	0.0
CHAR	12425	124	0.0	0.0	0.0	0.0	0.0
CHAR	12526	125	0.0	0.0	0.0	0.0	0.0
CHAR	12627	126	0.0	0.0	0.0	0.0	0.0
CHAR	12728	127	0.0	0.0	0.0	0.0	0.0
CHAR	12829	128	0.0	0.0	0.0	0.0	0.0
CHAR	12930	129	0.0	0.0	0.0	0.0	0.0
CHAR	13031	130	0.0	0.0	0.0	0.0	0.0
CHAR	13132	131	0.0	0.0	0.0	0.0	0.0
CHAR	13233	132	0.0	0.0	0.0	0.0	0.0
CHAR	13334	133	0.0	0.0	0.0	0.0	0.0
CHAR	13435	134	0.0	0.0	0.0	0.0	0.0
CHAR	13536	135	0.0	0.0	0.0	0.0	0.0
CHAR	13637	136	0.0	0.0	0.0	0.0	0.0
CHAR	13738	137	0.0	0.0	0.0	0.0	0.0
CHAR	13839	138	0.0	0.0	0.0	0.0	0.0
CHAR	13940	139	0.0	0.0	0.0	0.0	0.0
CHAR	14041	140	0.0	0.0	0.0	0.0	0.0
CHAR	14142	141	0.0	0.0	0.0	0.0	0.0
CHAR	14243	142	0.0	0.0	0.0	0.0	0.0
CHAR	14344	143	0.0	0.0	0.0	0.0	0.0
CHAR	14445	144	0.0	0.0	0.0	0.0	0.0
CHAR	14546	145	0.0	0.0	0.0	0.0	0.0
CHAR	14647	146	0.0	0.0	0.0	0.0	0.0
CHAR	14748	147	0.0	0.0	0.0	0.0	0.0
CHAR	14849	148	0.0	0.0	0.0	0.0	0.0
CHAR	14950	149	0.0	0.0	0.0	0.0	0.0
CHAR	15051	150	0.0	0.0	0.0	0.0	0.0
CHAR	15152	151	0.0	0.0	0.0	0.0	0.0
CHAR	15253	152	0.0	0.0	0.0	0.0	0.0
CHAR	15354	153	0.0	0.0	0.0	0.0	0.0
CHAR	15455	154	0.0	0.0	0.0	0.0	0.0
CHAR	15556	155	0.0	0.0	0.0	0.0	0.0
CHAR	15657	156	0.0	0.0	0.0	0.0	0.0
CHAR	15758	157	0.0	0.0	0.0	0.0	0.0
CHAR	15859	158	0.0	0.0	0.0	0.0	0.0
CHAR	15960	159	0.0	0.0	0.0	0.0	0.0
CHAR	16061	160	0.0	0.0	0.0	0.0	0.0
CHAR	16162	161	0.0	0.0	0.0	0.0	0.0
CHAR	16263	162	0.0	0.0	0.0	0.0	0.0
CHAR	16364	163	0.0	0.0	0.0	0.0	0.0
CHAR	16465	164	0.0	0.0	0.0	0.0	0.0
CHAR	16566	165	0.0	0.0	0.0	0.0	0.0
CHAR	16667	166	0.0	0.0	0.0	0.0	0.0
CHAR	16768	167	0.0	0.0	0.0	0.0	0.0
CHAR	16869	168	0.0	0.0	0.0	0.0	0.0
CHAR	16970	169	0.0	0.0	0.0	0.0	0.0
CHAR	17071	170	0.0	0.0	0.0	0.0	0.0
CHAR	17172	171	0.0	0.0	0.0	0.0	0.0
CHAR	17273	172	0.0	0.0	0.0	0.0	0.0
CHAR	17374	173	0.0	0.0	0.0	0.0	0.0
CHAR	17475	174	0.0	0.0	0.0	0.0	0.0
CHAR	17576	175	0.0	0.0	0.0	0.0	0.0
CHAR	17677	176	0.0	0.0	0.0	0.0	0.0
CHAR	17778	177	0.0	0.0	0.0	0.0	0.0
CHAR	17879	178	0.0	0.0	0.0	0.0	0.0
CHAR	17980	179	0.0	0.0	0.0	0.0	0.0
CHAR	18081	180	0.0	0.0	0.0	0.0	0.0
CHAR	18182	181	0.0	0.0	0.0	0.0	0.0
CHAR	18283	182	0.0	0.0	0.0	0.0	0.0
CHAR	18384	183	0.0	0.0	0.0	0.0	0.0
CHAR	18485	184	0.0	0.0	0.0	0.0	0.0
CHAR	18586	185	0.0	0.0	0.0	0.0	0.0
CHAR	18687	186	0.0	0.0	0.0	0.0	0.0
CHAR	18788	187	0.0	0.0	0.0	0.0	0.0
CHAR	18889	188	0.0	0.0	0.0	0.0	0.0
CHAR	18990	189	0.0	0.0	0.0	0.0	0.0
CHAR	19091	190	0.0	0.0	0.0	0.0	0.0

INPUT	BULK	DATA	DECK	F	C	H	U
1	2	3	4	5	6	7	8
PHAR 2324	1	1	35.54	1008.00	1150.10	428.36	10
PHAR 2425	1	1	38.50	182.6	5150.	113.6	
PHAR 2526	1	1	35.13	168.0	1000.	11.2	
PHAR 2627	1	1	32.70	132.0	1620.	69.0	
PHAR 2728	1	1	27.85	105.0	1340.	26.8	
PHAR 2829	1	1	25.45	72.0	660.	43.7	
PHAR 2930	1	1	1000.	5.5	5.5	11.0	
PHAR 3031	1	1	1000.	3.5	3.5	7.0	
PHAR 3132	1	1	1000.	2600.	454.	230.	
PHAR 3233	1	1	1000.	4250.	1031.	360.	
PHAR 3334	1	1	1000.	8250.	1485.	560.	
PHAR 3435	1	1	1000.	9912.	1683.	5150.	
PHAR 3536	1	1	1000.	8650.	1485.	560.	
PHAR 3637	1	1	1000.	4250.	1031.	360.	
PHAR 3738	1	1	1000.	2600.	454.	230.	
PHAR 3839	1	1	1000.	4250.	1031.	360.	
PHAR 3940	1	1	1000.	2600.	454.	230.	
PHAR 4041	1	1	25.81				
PELAS 1	28125.						
PELAS 2	28125.						
PELAS 3	4500.						
PELAS 4	20000.						
PHAR 5253	1	1	100.	72.	72.	144.	
PHAR 5354	1	1	100.	135.	135.	270.	
PHAR 5455	1	1	100.	120.	120.	240.	
MAT1	1	1	1.066				
CONM2 1	1	1	12.029				
CONM2 2	1	1	14.985				
CONM2 3	1	1	19.820				
CONM2 4	1	1	25.34				
CONM2 5	1	1	439.371				
CONM2 6	1	1	551.594				
CONM2 7	1	1	184.893				
CONM2 8	1	1	714.312				
CONM2 9	1	1	605.484				
CONM2 10	1	1	1.5.393				
CONM2 11	1	1	836.348				
CONM2 12	1	1	554.022				
CONM2 13	1	1	296.523				
CONM2 14	1	1	87.781				
CONM2 15	1	1	33.058				
CONM2 16	1	1	43.977				
CONM2 17	1	1	60.541				
CONM2 18	1	1	41.414				
CONM2 19	1	1	25.713				
CONM2 20	1	1	15.102				
CONM2 21	1	1	44.152				
CONM2 22	1	1	19.136				
CONM2 23	1	1	6.409				
CONM2 24	1	1	11.934				
CONM2 25	1	1	8.476				
CONM2 26	1	1	4.768				
CONM2 27	1	1	2.594				
CONM2 28	1	1	11.282				
CONM2 29	1	1	34.066				
CONM2 30	1	1	9.489				
CONM2 31	1	1	35.704				
CONM2 32	1	1	36.454				
CONM2 33	1	1	22.577				
CONM2 34	1	1	30.450				
CONM2 35	1	1	15.763				
CONM2 36	1	1	16.419				
CONM2 37	1	1	11.766				
CONM2 38	1	1	270.514				
CONM2 39	1	1	1.5.460				
CONM2 40	1	1					
CONM2 41	1	1					
CONM2 42	1	1					
CONM2 43	1	1					
CONM2 44	1	1					
CONM2 45	1	1					
CONM2 46	1	1					
CONM2 47	1	1					
CONM2 48	1	1					
CONM2 49	1	1					
CONM2 50	1	1					

CWT12

REPORT - AT DALLAS, TX 10001 - 735 VINT HUB SHEAR

[illegible]

TOTAL COUNT = 36

*** USE FOR INFORMATION MESSAGE 207. BULK DATA NOT SORTED, SORT WILL BE IN ORDER DECK.

PILOT SEAT RESPONSE TO 1000 LH 2/REV VERT HUM SHEAR

CARD COUNT	1	2	3	4	5	6	7	8	9	10
1- COAR	12	12	12	12	12	12	12	12	12	12
2- COAR	13	13	13	13	13	13	13	13	13	13
3- COAR	14	14	14	14	14	14	14	14	14	14
4- COAR	15	15	15	15	15	15	15	15	15	15
5- COAR	16	16	16	16	16	16	16	16	16	16
6- COAR	17	17	17	17	17	17	17	17	17	17
7- COAR	18	18	18	18	18	18	18	18	18	18
8- COAR	19	19	19	19	19	19	19	19	19	19
9- COAR	20	20	20	20	20	20	20	20	20	20
10- COAR	21	21	21	21	21	21	21	21	21	21
11- COAR	22	22	22	22	22	22	22	22	22	22
12- COAR	23	23	23	23	23	23	23	23	23	23
13- COAR	24	24	24	24	24	24	24	24	24	24
14- COAR	25	25	25	25	25	25	25	25	25	25
15- COAR	26	26	26	26	26	26	26	26	26	26
16- COAR	27	27	27	27	27	27	27	27	27	27
17- COAR	28	28	28	28	28	28	28	28	28	28
18- COAR	29	29	29	29	29	29	29	29	29	29
19- COAR	30	30	30	30	30	30	30	30	30	30
20- COAR	31	31	31	31	31	31	31	31	31	31
21- COAR	32	32	32	32	32	32	32	32	32	32
22- COAR	33	33	33	33	33	33	33	33	33	33
23- COAR	34	34	34	34	34	34	34	34	34	34
24- COAR	35	35	35	35	35	35	35	35	35	35
25- COAR	36	36	36	36	36	36	36	36	36	36
26- COAR	37	37	37	37	37	37	37	37	37	37
27- COAR	38	38	38	38	38	38	38	38	38	38
28- COAR	39	39	39	39	39	39	39	39	39	39
29- COAR	40	40	40	40	40	40	40	40	40	40
30- COAR	41	41	41	41	41	41	41	41	41	41
31- COAR	42	42	42	42	42	42	42	42	42	42
32- COAR	43	43	43	43	43	43	43	43	43	43
33- COAR	44	44	44	44	44	44	44	44	44	44
34- COAR	45	45	45	45	45	45	45	45	45	45
35- COAR	46	46	46	46	46	46	46	46	46	46
36- COAR	47	47	47	47	47	47	47	47	47	47
37- COAR	48	48	48	48	48	48	48	48	48	48
38- COAR	49	49	49	49	49	49	49	49	49	49
39- COAR	50	50	50	50	50	50	50	50	50	50
40- COAR	51	51	51	51	51	51	51	51	51	51
41- COAR	52	52	52	52	52	52	52	52	52	52
42- COAR	53	53	53	53	53	53	53	53	53	53
43- COAR	54	54	54	54	54	54	54	54	54	54
44- COAR	55	55	55	55	55	55	55	55	55	55
45- COAR	56	56	56	56	56	56	56	56	56	56
46- COAR	57	57	57	57	57	57	57	57	57	57
47- COAR	58	58	58	58	58	58	58	58	58	58
48- COAR	59	59	59	59	59	59	59	59	59	59
49- COAR	60	60	60	60	60	60	60	60	60	60
50- COAR	61	61	61	61	61	61	61	61	61	61
51- COAR	62	62	62	62	62	62	62	62	62	62
52- COAR	63	63	63	63	63	63	63	63	63	63
53- COAR	64	64	64	64	64	64	64	64	64	64
54- COAR	65	65	65	65	65	65	65	65	65	65
55- COAR	66	66	66	66	66	66	66	66	66	66
56- COAR	67	67	67	67	67	67	67	67	67	67
57- COAR	68	68	68	68	68	68	68	68	68	68
58- COAR	69	69	69	69	69	69	69	69	69	69
59- COAR	70	70	70	70	70	70	70	70	70	70
60- COAR	71	71	71	71	71	71	71	71	71	71
61- COAR	72	72	72	72	72	72	72	72	72	72
62- COAR	73	73	73	73	73	73	73	73	73	73
63- COAR	74	74	74	74	74	74	74	74	74	74
64- COAR	75	75	75	75	75	75	75	75	75	75
65- COAR	76	76	76	76	76	76	76	76	76	76
66- COAR	77	77	77	77	77	77	77	77	77	77
67- COAR	78	78	78	78	78	78	78	78	78	78
68- COAR	79	79	79	79	79	79	79	79	79	79
69- COAR	80	80	80	80	80	80	80	80	80	80
70- COAR	81	81	81	81	81	81	81	81	81	81
71- COAR	82	82	82	82	82	82	82	82	82	82
72- COAR	83	83	83	83	83	83	83	83	83	83

ELASTIC LINE MODEL OF THE AH-1G HELICOPTER
UNDAMPED FORCED RESPONSE STRAIN ENERGY METHOD
PILOT SEAT RESPONSE TO 1000 LB 2/REV VERT HUR SHEAR

CARD	COUNT	1	2	3	4	5	6	7	8	9	10	
73-	CONN2	1	12	12	12	12	12	12	12	12	12	
74-	CONN2	12	12	12	12	12	12	12	12	12	12	
75-	CONN2	12	12	12	12	12	12	12	12	12	12	
76-	CONN2	12	12	12	12	12	12	12	12	12	12	
77-	CONN2	12	12	12	12	12	12	12	12	12	12	
78-	CONN2	12	12	12	12	12	12	12	12	12	12	
79-	CONN2	12	12	12	12	12	12	12	12	12	12	
80-	CONN2	12	12	12	12	12	12	12	12	12	12	
81-	CONN2	12	12	12	12	12	12	12	12	12	12	
82-	CONN2	12	12	12	12	12	12	12	12	12	12	
83-	CONN2	12	12	12	12	12	12	12	12	12	12	
84-	CONN2	12	12	12	12	12	12	12	12	12	12	
85-	CONN2	12	12	12	12	12	12	12	12	12	12	
86-	CONN2	12	12	12	12	12	12	12	12	12	12	
87-	CONN2	12	12	12	12	12	12	12	12	12	12	
88-	CONN2	12	12	12	12	12	12	12	12	12	12	
89-	CONN2	12	12	12	12	12	12	12	12	12	12	
90-	CONN2	12	12	12	12	12	12	12	12	12	12	
91-	CONN2	12	12	12	12	12	12	12	12	12	12	
92-	CONN2	12	12	12	12	12	12	12	12	12	12	
93-	CONN2	12	12	12	12	12	12	12	12	12	12	
94-	CONN2	12	12	12	12	12	12	12	12	12	12	
95-	CONN2	12	12	12	12	12	12	12	12	12	12	
96-	CONN2	12	12	12	12	12	12	12	12	12	12	
97-	CONN2	12	12	12	12	12	12	12	12	12	12	
98-	CONN2	12	12	12	12	12	12	12	12	12	12	
99-	CONN2	12	12	12	12	12	12	12	12	12	12	
100-	CONN2	12	12	12	12	12	12	12	12	12	12	
101-	CONN2	12	12	12	12	12	12	12	12	12	12	
102-	CONN2	12	12	12	12	12	12	12	12	12	12	
103-	CONN2	12	12	12	12	12	12	12	12	12	12	
104-	CONN2	12	12	12	12	12	12	12	12	12	12	
105-	CONN2	12	12	12	12	12	12	12	12	12	12	
106-	CONN2	12	12	12	12	12	12	12	12	12	12	
107-	CONN2	12	12	12	12	12	12	12	12	12	12	
108-	CONN2	12	12	12	12	12	12	12	12	12	12	
109-	CONN2	12	12	12	12	12	12	12	12	12	12	
110-	CONN2	12	12	12	12	12	12	12	12	12	12	
111-	CONN2	12	12	12	12	12	12	12	12	12	12	
112-	CONN2	12	12	12	12	12	12	12	12	12	12	
113-	CONN2	12	12	12	12	12	12	12	12	12	12	
114-	CONN2	12	12	12	12	12	12	12	12	12	12	
115-	CONN2	12	12	12	12	12	12	12	12	12	12	
116-	CONN2	12	12	12	12	12	12	12	12	12	12	
117-	CONN2	12	12	12	12	12	12	12	12	12	12	
118-	CONN2	12	12	12	12	12	12	12	12	12	12	
119-	CONN2	12	12	12	12	12	12	12	12	12	12	
120-	CONN2	12	12	12	12	12	12	12	12	12	12	
121-	CONN2	12	12	12	12	12	12	12	12	12	12	
122-	CONN2	12	12	12	12	12	12	12	12	12	12	
123-	CONN2	12	12	12	12	12	12	12	12	12	12	
124-	CONN2	12	12	12	12	12	12	12	12	12	12	
125-	CONN2	12	12	12	12	12	12	12	12	12	12	
126-	CONN2	12	12	12	12	12	12	12	12	12	12	
127-	CONN2	12	12	12	12	12	12	12	12	12	12	
128-	CONN2	12	12	12	12	12	12	12	12	12	12	
129-	CONN2	12	12	12	12	12	12	12	12	12	12	
130-	CONN2	12	12	12	12	12	12	12	12	12	12	
131-	CONN2	12	12	12	12	12	12	12	12	12	12	
132-	CONN2	12	12	12	12	12	12	12	12	12	12	
133-	CONN2	12	12	12	12	12	12	12	12	12	12	
134-	CONN2	12	12	12	12	12	12	12	12	12	12	
135-	CONN2	12	12	12	12	12	12	12	12	12	12	
136-	CONN2	12	12	12	12	12	12	12	12	12	12	
137-	CONN2	12	12	12	12	12	12	12	12	12	12	
138-	CONN2	12	12	12	12	12	12	12	12	12	12	
139-	CONN2	12	12	12	12	12	12	12	12	12	12	
140-	CONN2	12	12	12	12	12	12	12	12	12	12	
141-	CONN2	12	12	12	12	12	12	12	12	12	12	
142-	CONN2	12	12	12	12	12	12	12	12	12	12	
143-	CONN2	12	12	12	12	12	12	12	12	12	12	
144-	CONN2	12	12	12	12	12	12	12	12	12	12	

CARD COUNT	I	2	3	4	5	6	7	8	9	10	T/R HUB
145	GRID	22	442.24	.0	57.20						
146	GRID	23	442.15	.0	53.50						
147	GRID	24	464.10	.0	59.80						
148	GRID	25	480.23	.0	75.40						
149	GRID	26	469.93	.0	81.52						
150	GRID	27	506.77	.0	102.61						
151	GRID	28	515.43	.0	104.46						
152	GRID	29	520.67	.0	118.27						
153	GRID	30	520.67	7.20	118.27						
154	GRID	31	520.67	14.10	118.27						
155	GRID	32	193.858	-50.0	62.246						
156	GRID	33	136.574	-42.5	61.226						
157	GRID	34	194.230	-30.0	60.498						
158	GRID	35	182.202	-19.14	59.868						
159	GRID	36	182.202	19.14	59.868						
160	GRID	37	176.523	42.0	61.226						
161	GRID	38	176.523	42.0	61.226						
162	GRID	39	199.894	60.0	62.246						
163	GRID	40	199.894	60.0	62.246						
164	GRID	41	149.94	-12.375	77.57						
165	GRID	42	149.94	12.375	77.57						
166	GRID	43	211.72	-12.375	77.57						
167	GRID	44	211.72	12.375	77.57						
168	GRID	45	214.50	.0	77.57						
169	GRID	46	183.94	-12.375	77.57						
170	GRID	47	183.94	12.375	77.57						
171	GRID	48	211.72	-12.375	77.57						
172	GRID	49	211.72	12.375	77.57						
173	GRID	50	214.50	.0	77.57						
174	GRID	51	200.	.0	83.8						
175	GRID	52	200.	.0	77.2						
176	GRID	53	200.	.0	98.0						
177	GRID	54	200.	.0	115.0						
178	GRID	55	200.	.0	153.0						
179	GRID	60	248.0	.0	86.0						
180	GRID	60	1.064	.0							
181	GRID	60	1.064	.0							
182	GRID	60	1.064	.0							
183	GRID	12	1000.	1650.	250.	200.					
184	GRID	13	1000.	1300.	700.	200.					
185	GRID	14	1000.	5350.	1100.	200.					
186	GRID	15	1000.	5400.	1100.	255.					
187	GRID	16	1000.	7300.	2750.	850.					
188	GRID	17	1000.	7300.	3000.	850.					
189	GRID	18	1000.	7300.	3200.	2000.					
190	GRID	19	1000.	9750.	8200.	2000.					
191	GRID	20	1000.	12750.	14710.	3250.					
192	GRID	21	1000.	19000.	14710.	3150.					
193	GRID	22	1000.	2912.	16410.	5150.					
194	GRID	1314	1000.	13900.	11670.	2000.					
195	GRID	1415	1								

66

ELASTIC LINE MODEL OF THE AH-1G HELICOPTER
UNDAMPED FORCED RESPONSE - STRAIN ENERGY METHOD
PILOT SEAT RESPONSE TO 1000 G 2/REV VERT HUB SHEAR

CARD	1	2	3	4	5	6	7	8	9	10
117-	PIA1	1612	1	1000.	9012.	1683.	5150.			
118-	PIA2	1738	1	1000.	4250.	1485.	560.			
119-	PIA3	3839	1	1000.	4250.	1031.	380.			
120-	PIA4	3940	1	1000.	2000.	454.	230.			
121-	PIA5	5112	1	25.81	72.	72.	144.			
122-	PIA6	3223	1	100.	135.	135.	270.			
123-	PIA7	3223	1	100.	120.	120.	240.			
124-	PIA8	3055	1	100.						
125-	PELAS	1	28125.							
126-	PELAS	2	28125.							
127-	PELAS	3	4500.							
128-	PELAS	33	20000.							
129-	RELAD2	1000	553	0	0	99	0			
130-	TATU01	99		0	0	1.0	1.0	END		
131-	ENDATA	0.0	1.0	200.0	1.0					CRPFC

1. VOL. 2.0 NASTCAN MAG COMPILER - 40000 LISTING.

NOTES ON THE EFFECTS OF THE
CIVIL SERVICE REFORMS
ON THE ECONOMY OF THE
UNITED STATES

68

ELASTIC LINE MODEL OF THE AH-1G HELICOPTER
UNIAXIALLY FORCED RESPONSE STRAIN ENERGY METHOD
PILOT SEAT RESPONSE TO 1000 LB Z/REV VERT HUR SHEAR
LEVEL 2.0 NASTRAN DHAP COMPILER - SOURCE LISTING

```

66 CHKONT KGG $
67 LABEL LBL11 $
68 PARAM //C,N,MPY/V,N,NCKIP/C,N,O/C,N,O $
69 V04 CASECCAGE044,EDFXTIN,SIL,GPDT,4GPDT,CSM/RG,USE,ASET/, V,N,
LUSSET/V,N,MPCF1/V,N,MPCF2/V,N,SINGLE/V,N,OMIT/V,N,REACT/V,N,
NSKIP/V,N,REPEAT/V,N,NUSET/V,N,NOL/V,N,NOA/C,V,5UNIT $
70 SAVE MPCF1,SINGLE,OMIT,NUSET,REACT,MPCF2,NSKIP,REPEAT,NOL,NOA $
71 PURGE GM,GMD/MPCF1/GD,GUD/OMIT/KFS,PSF,OPC,NUSET $
72 CHKONT GM,GMD,RG,GD,GUD,KFS,PSF,OPC,NUSET $
73 CIND LBL4,GENEL $
74 CIND LBL4,NDSIMP $
75 GPOD GPL,GPST,NUSET,SIL/USPST/V,N,MGPST $
76 SAVE NUGPST $
77 CIND LBL4,NUGPST $
78 DEF OGPST,,,,, $
79 LABEL LBL4 $
80 EQUIV KGG,KNN/MPCF1/MGG,MNN/MPCF1/ RGG,9NN/MPCF1/KAGG,KANN/MPCF1 $
81 CHKONT KNN,MNN,9NN,KANN $
82 CIND LBL2,MPCF1 $
83 MCF1 USET,RG/GM $
84 CHKONT GM $
85 MCF2 USET,CM,KGS,MGS,PSG,KAGG/KNN,MNN,9NN,KANN $
86 CHKONT KNN,MNN,9NN,KANN $
87 LABEL LBL2 $
88 EQUIV KNN,KFF/SINGLE/S/MNN,MFF/SINGLE/9NN,9FF/SINGLE/KANN,KAFF/SINGLE $
89 CHKONT KFF,MFF,9FF,KAFF $
90 CIND LBL3,SINGLE $
91 MCF1 USET,KNN,MNN,9NN,KANN/KFF,KFS,MFF,9FF,KAFF $
92 CHKONT KFS,KFF,MFF,9FF,KAFF $
93 LABEL LBL3 $
94 EQUIV KFF,KAA/OMIT $
95 EQUIV MFF,MAA/OMIT $
96 EQUIV 9FF,9AA/OMIT $
97 EQUIV KAFF,KAAA/OMIT $
98 CHKONT KAA,MAA,9AA,KAAA $
99 CIND LBL5,OMIT $
100 SAVE USET,KFF,,,,,KGG,KAGG,KNN,KANN,KFF,,,,, $

```


ELASTIC LINE MODEL OF THE AH-1G HELICOPTER
 UNWEIGHTED FORCED RESPONSE STRAIN ENERGY METHOD
 PILOT SEAT RESPONSE TO 1000 L4 2/REV VERT HUM SHEAR
 LEVEL 2.0 NASTRAN DMAP COMPILER SOURCE LISTING

APRIL 4, 1979 NASTRAN 1/17/77 PAGE 18

201 END

*** ERRORS FOUND - EXECUTE NASTRAN PROGRAM ***

*** SYSTEM INFORMATION MESSAGE 3113. EMGPRD PROCESSING DOUBLE PRECISION ELEMENTS OF TYPE 3A STARTING WITH ID 12
 *** SYSTEM INFORMATION MESSAGE 3107. EMGOLD IS PROCESSING ELEMENTS OF TYPE # 3A BEGINNING WITH ELEMENT ID # 12
 *** SYSTEM INFORMATION MESSAGE 3113. EMGPRD PROCESSING DOUBLE PRECISION ELEMENTS OF TYPE 11 STARTING WITH ID 41461
 *** SYSTEM INFORMATION MESSAGE 3113. EMGPRD PROCESSING DOUBLE PRECISION ELEMENTS OF TYPE 30 STARTING WITH ID 1
 *** SYSTEM INFORMATION MESSAGE 3107. EMGOLD IS PROCESSING ELEMENTS OF TYPE # 30 BEGINNING WITH ELEMENT ID # 1

ELASTIC LINE MODEL OF THE AH-1G HELICOPTER
 UNDAMPED FORCED RESPONSE STRAIN ENERGY METHOD
 WITH SEAT RESPONSE TO 1000 LBS PARV VERT HMM SHIP

ADVAL 00 1070 WASTMAN 1/17/77 PAGE 19

*** USED WARNING MESSAGE 3041
 EXTERNAL GRID POINT 0 DOES NOT EXIST OR IS NOT A GEOMETRIC GRID POINT.
 THE BASIC ORIGIN WILL BE USED.

ELASTIC LINE MODEL OF THE AH-1G HELICOPTER
UNOAKED FORCED RESPONSE STRAIN ENERGY METHOD
PILOT SEAT RESPONSE TO 1000 LB 2/REV VERT HUR SHEAR

*** UOOF WARNING MESSAGE 3017

ONE OR MORE POTENTIAL SINGULARITIES HAVE NOT BEEN REMOVED BY SINGLE OR MULTI-POINT CONSTRAINTS.

LOAD LINE MODEL OF THE M-16 HELICOPTER
 UNLOAD COUPLED RESPONSE STRAIN ENERGY METHOD

APRIL 4, 1979 NASTRAN 1/17/77 PAGE 22

PILLOT SEAT RESPONSE TO 1000 LB 2/REV VERT HUB SHEAR

POINT ID.	TYPE	SINGULARITY ORDER	G R I D	P O I N T	S I N G U L A R I T Y	T A B L E	SPC	WEAKEST COMBINATION	WEAKEST COMBINATION
51	G	2	2	2	2	2	2	2	2
51	G	2	4	4	4	4	4	4	4
51	G	2	6	6	6	6	6	6	6

***** INFORMATION MESSAGE 30/3--PARAMETERS FOR SYMMETRIC DECOMPOSITION OF DATA BLOCK SCRATCH9 X N # 254 <
 TIME ESTIMATE # 1 C AVG # 18 PC AVG # 0 SPILL GROUPS # 0 S AVG # 1
 ADDITIONAL CORE # -60050 C MAX # 29 PC MAX # 0 PC GROUPS # 0 PREFACE LINES # 1

POINT ID.	TYPE	T1	T2	T3	R1	R2	R3
1	G	4.874033E-05	7.544444E-04	2.240049E-03	-1.990273E-05	8.833830E-05	-7.553022E-06
2	G	4.874033E-05	7.544444E-04	1.671908E-03	-1.990273E-05	8.833830E-05	-7.553022E-06
3	G	4.874033E-05	7.544444E-04	3.263431E-04	-1.990273E-05	8.833830E-05	-7.553022E-06
4	G	4.874033E-05	7.544444E-04	8.833830E-05	-1.990273E-05	8.833830E-05	-7.553022E-06
5	G	4.874033E-05	7.544444E-04	8.833830E-05	-1.990273E-05	8.833830E-05	-7.553022E-06
6	G	4.874033E-05	7.544444E-04	8.833830E-05	-1.990273E-05	8.833830E-05	-7.553022E-06
7	G	4.874033E-05	7.544444E-04	8.833830E-05	-1.990273E-05	8.833830E-05	-7.553022E-06
8	G	4.874033E-05	7.544444E-04	8.833830E-05	-1.990273E-05	8.833830E-05	-7.553022E-06
9	G	4.874033E-05	7.544444E-04	8.833830E-05	-1.990273E-05	8.833830E-05	-7.553022E-06
10	G	4.874033E-05	7.544444E-04	8.833830E-05	-1.990273E-05	8.833830E-05	-7.553022E-06
11	G	4.874033E-05	7.544444E-04	8.833830E-05	-1.990273E-05	8.833830E-05	-7.553022E-06
12	G	4.874033E-05	7.544444E-04	8.833830E-05	-1.990273E-05	8.833830E-05	-7.553022E-06
13	G	4.874033E-05	7.544444E-04	8.833830E-05	-1.990273E-05	8.833830E-05	-7.553022E-06
14	G	4.874033E-05	7.544444E-04	8.833830E-05	-1.990273E-05	8.833830E-05	-7.553022E-06
15	G	4.874033E-05	7.544444E-04	8.833830E-05	-1.990273E-05	8.833830E-05	-7.553022E-06
16	G	4.874033E-05	7.544444E-04	8.833830E-05	-1.990273E-05	8.833830E-05	-7.553022E-06
17	G	4.874033E-05	7.544444E-04	8.833830E-05	-1.990273E-05	8.833830E-05	-7.553022E-06
18	G	4.874033E-05	7.544444E-04	8.833830E-05	-1.990273E-05	8.833830E-05	-7.553022E-06
19	G	4.874033E-05	7.544444E-04	8.833830E-05	-1.990273E-05	8.833830E-05	-7.553022E-06
20	G	4.874033E-05	7.544444E-04	8.833830E-05	-1.990273E-05	8.833830E-05	-7.553022E-06
21	G	4.874033E-05	7.544444E-04	8.833830E-05	-1.990273E-05	8.833830E-05	-7.553022E-06
22	G	4.874033E-05	7.544444E-04	8.833830E-05	-1.990273E-05	8.833830E-05	-7.553022E-06
23	G	4.874033E-05	7.544444E-04	8.833830E-05	-1.990273E-05	8.833830E-05	-7.553022E-06
24	G	4.874033E-05	7.544444E-04	8.833830E-05	-1.990273E-05	8.833830E-05	-7.553022E-06

POINT ID.	TYPE	T1	T2	T3	R1	R2	R3
1	G	3.03997E-05 0.0	7.37409E-04 0.0	1.54477E-03 0.0	-1.93484E-05 0.0	7.90448E-05 0.0	-7.35298E-06 0.0
2	G	3.03997E-05 0.0	6.99618E-04 0.0	1.03099E-03 0.0	-1.93484E-05 0.0	7.90448E-05 0.0	-7.35163E-06 0.0
3	G	3.03997E-05 0.0	5.77600E-04 0.0	1.73363E-04 0.0	-1.93484E-05 0.0	7.90448E-05 0.0	-7.33458E-06 0.0
4	G	3.03997E-05 0.0	4.76948E-04 0.0	1.25688E-03 0.0	-1.93484E-05 0.0	7.90448E-05 0.0	-7.29986E-06 0.0
5	G	-1.01637E-03 0.0	6.69824E-05 0.0	-1.29624E-03 0.0	-1.93484E-05 0.0	7.90448E-05 0.0	-7.29986E-06 0.0
6	G	3.03997E-05 0.0	3.40505E-04 0.0	-2.66120E-03 0.0	-1.93484E-05 0.0	7.90448E-05 0.0	-7.17214E-06 0.0
7	G	3.03997E-05 0.0	2.02078E-04 0.0	-4.26304E-03 0.0	-1.93484E-05 0.0	7.90448E-05 0.0	-6.87858E-06 0.0
8	G	3.03997E-05 0.0	8.22540E-05 0.0	-5.72571E-03 0.0	-1.93484E-05 0.0	7.90448E-05 0.0	-6.39477E-06 0.0
9	G	3.03997E-05 0.0	2.91947E-05 0.0	-6.55848E-03 0.0	-1.93484E-05 0.0	7.90448E-05 0.0	-6.08017E-06 0.0
10	G	3.03997E-05 0.0	-2.13322E-05 0.0	-7.21984E-03 0.0	-1.93484E-05 0.0	7.90448E-05 0.0	-5.80127E-06 0.0
11	G	3.03997E-05 0.0	-2.33460E-04 0.0	-1.12637E-02 0.0	-1.93484E-05 0.0	7.90448E-05 0.0	-4.29333E-06 0.0
12	G	3.03997E-05 0.0	-2.62710E-04 0.0	-1.20281E-02 0.0	-2.00033E-05 0.0	1.11573E-04 0.0	-4.06202E-06 0.0
13	G	3.03997E-05 0.0	-3.23121E-04 0.0	-1.38943E-02 0.0	-1.86132E-05 0.0	1.20297E-04 0.0	-3.47851E-06 0.0
14	G	3.03997E-05 0.0	-4.16844E-04 0.0	-1.83411E-02 0.0	-1.51164E-05 0.0	1.13410E-04 0.0	-1.56486E-06 0.0
15	G	3.03997E-05 0.0	-4.36844E-04 0.0	-2.10429E-02 0.0	-1.19872E-05 0.0	8.55562E-05 0.0	9.05942E-06 0.0
16	G	4.29923E-06 0.0	-4.18637E-04 0.0	-2.26403E-02 0.0	-8.73557E-06 0.0	5.56036E-05 0.0	1.86527E-06 0.0
17	G	2.06663E-05 0.0	-3.53829E-04 0.0	-2.33251E-02 0.0	-6.95990E-06 0.0	1.95582E-05 0.0	4.27257E-06 0.0
18	G	2.06663E-05 0.0	-2.27200E-04 0.0	-2.33087E-02 0.0	-4.05183E-06 0.0	-2.10755E-05 0.0	7.13061E-06 0.0
19	G	-8.37990E-05 0.0	-3.70222E-05 0.0	-2.23108E-02 0.0	-3.01786E-07 0.0	-7.41350E-05 0.0	1.07378E-05 0.0
20	G	-2.51080E-04 0.0	2.26825E-04 0.0	-2.00245E-02 0.0	4.01929E-06 0.0	-1.43733E-04 0.0	1.46943E-05 0.0
21	G	-5.22410E-04 0.0	5.08017E-04 0.0	-1.00491E-02 0.0	1.09868E-05 0.0	-2.34965E-04 0.0	1.88231E-05 0.0
22	G	-9.22307E-04 0.0	9.15979E-04 0.0	-1.00282E-02 0.0	1.90652E-05 0.0	-3.36502E-04 0.0	2.34700E-05 0.0
23	G	-1.44040E-03 0.0	1.41099E-03 0.0	-1.06770E-03 0.0	3.03413E-05 0.0	-4.26764E-04 0.0	2.91123E-05 0.0
24	G	-2.01001E-03 0.0	2.14040E-03 0.0	9.08913E-03 0.0	4.71484E-05 0.0	-2.67091E-04 0.0	3.03010E-05 0.0

POINT ID	TYPE	T1	T2	T3	R1	R2	R3
25	G	-1.11739E-02 0.0	1.466181E-03 0.0	1.440861E-02 0.0	1.127584E-04 0.0	-5.469644E-04 0.0	4.547995E-05 0.0
26	G	-1.620710E-02 0.0	1.632145E-03 0.0	2.361178E-02 0.0	1.622661E-04 0.0	-6.079494E-04 0.0	1.400797E-04 0.0
27	G	-2.134800E-02 0.0	1.666117E-03 0.0	2.907395E-02 0.0	2.214033E-04 0.0	-6.265406E-04 0.0	1.934432E-04 0.0
28	G	-2.603804E-02 0.0	1.464486E-03 0.0	3.466991E-02 0.0	2.929114E-04 0.0	-6.336772E-04 0.0	2.584504E-04 0.0
29	G	-3.241610E-02 0.0	1.219792E-03 0.0	4.037144E-02 0.0	3.767423E-04 0.0	-6.501069E-04 0.0	3.345830E-04 0.0
30	G	-3.481665E-02 0.0	4.989358E-04 0.0	4.376986E-02 0.0	4.156823E-04 0.0	-6.532557E-04 0.0	3.698836E-04 0.0
31	G	-4.08377E-02 0.0	4.989377E-04 0.0	4.678277E-02 0.0	4.777317E-04 0.0	-6.532557E-04 0.0	4.240485E-04 0.0
32	G	-4.431943E-02 0.0	4.989391E-04 0.0	5.072388E-02 0.0	6.178971E-04 0.0	-6.532557E-04 0.0	5.465662E-04 0.0
33	G	1.165710E-03 0.0	4.465312E-05 0.0	-1.148170E-02 0.0	-1.253787E-05 0.0	1.121787E-04 0.0	-3.951713E-06 0.0
34	G	1.120494E-03 0.0	4.494841E-05 0.0	-1.133533E-02 0.0	-1.298460E-05 0.0	1.120947E-04 0.0	-3.955556E-06 0.0
35	G	1.008043E-03 0.0	4.448064E-05 0.0	-1.123883E-02 0.0	-1.337882E-05 0.0	1.119525E-04 0.0	-3.967531E-06 0.0
36	G	1.060496E-03 0.0	4.580966E-05 0.0	-1.116608E-02 0.0	-1.491748E-05 0.0	1.117308E-04 0.0	-3.977905E-06 0.0
37	G	1.217054E-03 0.0	4.580931E-05 0.0	-1.194101E-02 0.0	-2.6574705E-05 0.0	1.117561E-04 0.0	-4.166935E-06 0.0
38	G	1.332711E-03 0.0	3.758240E-05 0.0	-1.245458E-02 0.0	-2.711693E-05 0.0	1.120140E-04 0.0	4.184752E-06 0.0
39	G	1.464774E-03 0.0	2.672098E-05 0.0	-1.306318E-02 0.0	-2.800896E-05 0.0	1.121824E-04 0.0	4.202487E-06 0.0
40	G	1.604886E-03 0.0	1.221654E-05 0.0	-1.392617E-02 0.0	-2.865977E-05 0.0	1.122644E-04 0.0	4.208870E-06 0.0
41	G	3.402717E-03 0.0	3.175149E-04 0.0	-1.094291E-02 0.0	-2.4000533E-05 0.0	1.115734E-04 0.0	4.0662023E-06 0.0
42	G	3.413252E-03 0.0	3.175149E-04 0.0	-1.148804E-02 0.0	-2.4000533E-05 0.0	1.115734E-04 0.0	4.0662023E-06 0.0
43	G	3.602717E-03 0.0	2.2790941E-04 0.0	-1.342294E-02 0.0	-2.4000533E-05 0.0	1.115734E-04 0.0	4.0662023E-06 0.0
44	G	3.614252E-03 0.0	2.2790941E-04 0.0	-1.391811E-02 0.0	-2.4000533E-05 0.0	1.115734E-04 0.0	4.0662023E-06 0.0
45	G	3.811756E-03 0.0	2.8177517E-04 0.0	-1.396077E-02 0.0	-2.4000533E-05 0.0	1.115734E-04 0.0	4.0662023E-06 0.0
46	G	3.977314E-03 0.0	3.402706E-04 0.0	-1.234166E-02 0.0	-2.402498E-06 0.0	1.115734E-04 0.0	4.0662023E-06 0.0
47	G	3.989971E-03 0.0	3.410273E-04 0.0	-1.241666E-02 0.0	-2.402498E-06 0.0	1.115734E-04 0.0	4.0662023E-06 0.0
48	G	3.923145E-03 0.0	2.402706E-04 0.0	-1.031100E-02 0.0	-2.402498E-06 0.0	1.115734E-04 0.0	4.0662023E-06 0.0

ELASTIC LINE MODEL OF THE AH-1G HELICOPTER
UNLOADED FORCED RESPONSE STRAIN ENERGY METHOD
PILOT SEAT RESPONSE TO 1000 LBS 2/REV VERT HUR SHARP
FOR JUMP # 1.000000E+01

POINT NO.	TYPE	T1	T2	T3	R1	R2	R3
49	G	3.342921E-03 0.0	2.409487E-04 0.0	-1.043543E-02 0.0	-5.024988E-06 0.0	-7.323143E-05 0.0	-4.099636E-06 0.0
50	G	3.262186E-03 0.0	2.295517E-04 0.0	-1.011408E-02 0.0	-5.024988E-06 0.0	-7.323143E-05 0.0	-4.099636E-06 0.0
51	G	2.701357E-03 0.0	3.203021E-04 0.0	-1.146594E-02 0.0	-5.024988E-06 0.0	-7.323143E-05 0.0	-4.099636E-06 0.0
52	G	3.316684E-03 0.0	2.871372E-04 0.0	-1.146594E-02 0.0	-5.024988E-06 0.0	-7.323143E-05 0.0	-4.099636E-06 0.0
53	G	1.311471E-03 0.0	3.916568E-04 0.0	-1.129531E-02 0.0	3.405797E-07 0.0	-6.145172E-05 0.0	-4.099636E-06 0.0
54	G	6.450893E-04 0.0	3.302987E-04 0.0	-1.114966E-02 0.0	6.638805E-06 0.0	-2.703117E-05 0.0	-4.099636E-06 0.0
55	G	4.874486E-04 0.0	4.066260E-05 0.0	-1.081774E-02 0.0	1.365370E-05 0.0	7.273181E-06 0.0	-4.099636E-06 0.0
56	G	4.116551E-03 0.0	1.304774E-04 0.0	-1.811508E-02 0.0	-1.511448E-05 0.0	1.134100E-04 0.0	-1.504861E-06 0.0

*** USER WARNING MESSAGE 2354.
GAPJUMPJUMP IS UNABLE TO CONTINUE AND HAS BEEN TERMINATED DUE TO ERROR MESSAGE PRINTED ABOVE OR BELOW THIS MESSAGE.
THIS ERROR OCCURRED IN GAPJUMP CODE WHERE THE VARIABLE -INPROB- WAS SET # 20

ELASTIC LINE MODEL OF THE AH-1G HELICOPTER
 UNDAMPED FORCED RESPONSE STRAIN ENERGY METHOD
 PILOT SEAT RESPONSE TO 1000 L/3 2/REV VERT HUB SHEAR

APRIL 4, 1979 NASTHAN 1/17/77 PAGE 29

*** SYSTEM WARNING MESSAGE 3002

EUF ENCOUNTERED WHILE READING DATA SET SCRATCH3XFILE 3036 IN SUBROUTINE GPFDR

PLASTIC LINE MODEL OF THE 44-16 HELICOPTER
UNDAMPED FORCED RESPONSE, STRAIN ENERGY METHOD
PILOT SEAT RESPONSE TO 1000 LH 2/REV VERT HUR SHEAR

E L E M E N T S T A I N E N E R G I E S			
ELEMENT-1	TYPE	* RAR	* TOTAL FIRM ALL TYPES
12	12	12	12
23	23	23	23
34	34	34	34
40	40	40	40
57	57	57	57
60	60	60	60
910	910	910	910
1011	1011	1011	1011
1112	1112	1112	1112
1237	1237	1237	1237
1334	1334	1334	1334
1415	1415	1415	1415
1516	1516	1516	1516
1717	1717	1717	1717
1819	1819	1819	1819
1920	1920	1920	1920
2021	2021	2021	2021
2122	2122	2122	2122
2223	2223	2223	2223
2324	2324	2324	2324
2425	2425	2425	2425
2526	2526	2526	2526
2627	2627	2627	2627
2728	2728	2728	2728
2829	2829	2829	2829
2930	2930	2930	2930
3031	3031	3031	3031
3132	3132	3132	3132
3233	3233	3233	3233
3334	3334	3334	3334
3435	3435	3435	3435
3536	3536	3536	3536
3637	3637	3637	3637
3738	3738	3738	3738
3839	3839	3839	3839
3940	3940	3940	3940
4041	4041	4041	4041
4142	4142	4142	4142
4243	4243	4243	4243
4344	4344	4344	4344
4445	4445	4445	4445
4546	4546	4546	4546
4647	4647	4647	4647
4748	4748	4748	4748
4849	4849	4849	4849
4950	4950	4950	4950
5051	5051	5051	5051
5152	5152	5152	5152
5253	5253	5253	5253
5354	5354	5354	5354
5455	5455	5455	5455
5556	5556	5556	5556
5657	5657	5657	5657
5758	5758	5758	5758
5859	5859	5859	5859
5960	5960	5960	5960
6061	6061	6061	6061
6162	6162	6162	6162
6263	6263	6263	6263
6364	6364	6364	6364
6465	6465	6465	6465
6566	6566	6566	6566
6667	6667	6667	6667
6768	6768	6768	6768
6869	6869	6869	6869
6970	6970	6970	6970
7071	7071	7071	7071
7172	7172	7172	7172
7273	7273	7273	7273
7374	7374	7374	7374
7475	7475	7475	7475
7576	7576	7576	7576
7677	7677	7677	7677
7778	7778	7778	7778
7879	7879	7879	7879
7980	7980	7980	7980
8081	8081	8081	8081
8182	8182	8182	8182
8283	8283	8283	8283
8384	8384	8384	8384
8485	8485	8485	8485
8586	8586	8586	8586
8687	8687	8687	8687
8788	8788	8788	8788
8889	8889	8889	8889
8990	8990	8990	8990
9091	9091	9091	9091
9192	9192	9192	9192
9293	9293	9293	9293
9394	9394	9394	9394
9495	9495	9495	9495
9596	9596	9596	9596
9697	9697	9697	9697
9798	9798	9798	9798
9899	9899	9899	9899
9900	9900	9900	9900
10001	10001	10001	10001
10002	10002	10002	10002
10003	10003	10003	10003
10004	10004	10004	10004
10005	10005	10005	10005
10006	10006	10006	10006
10007	10007	10007	10007
10008	10008	10008	10008
10009	10009	10009	10009
10010	10010	10010	10010
10011	10011	10011	10011
10012	10012	10012	10012
10013	10013	10013	10013
10014	10014	10014	10014
10015	10015	10015	10015
10016	10016	10016	10016
10017	10017	10017	10017
10018	10018	10018	10018
10019	10019	10019	10019
10020	10020	10020	10020
10021	10021	10021	10021
10022	10022	10022	10022
10023	10023	10023	10023
10024	10024	10024	10024
10025	10025	10025	10025
10026	10026	10026	10026
10027	10027	10027	10027
10028	10028	10028	10028
10029	10029	10029	10029
10030	10030	10030	10030
10031	10031	10031	10031
10032	10032	10032	10032
10033	10033	10033	10033
10034	10034	10034	10034
10035	10035	10035	10035
10036	10036	10036	10036
10037	10037	10037	10037
10038	10038	10038	10038
10039	10039	10039	10039
10040	10040	10040	10040
10041	10041	10041	10041
10042	10042	10042	10042
10043	10043	10043	10043
10044	10044	10044	10044
10045	10045	10045	10045
10046	10046	10046	10046
10047	10047	10047	10047
10048	10048	10048	10048
10049	10049	10049	10049
10050	10050	10050	10050
10051	10051	10051	10051
10052	10052	10052	10052
10053	10053	10053	10053
10054	10054	10054	10054
10055	10055	10055	10055
10056	10056	10056	10056
10057	10057	10057	10057
10058	10058	10058	10058
10059	10059	10059	10059
10060	10060	10060	10060
10061	10061	10061	10061
10062	10062	10062	10062
10063	10063	10063	10063
10064	10064	10064	10064
10065	10065	10065	10065
10066	10066	10066	10066
10067	10067	10067	10067
10068	10068	10068	10068
10069	10069	10069	10069
10070	10070	10070	10070
10071	10071	10071	10071
10072	10072	10072	10072
10073	10073	10073	10073
10074	10074	10074	10074
10075	10075	10075	10075
10076	10076	10076	10076
10077	10077	10077	10077
10078	10078	10078	10078
10079	10079	10079	10079
10080	10080	10080	10080
10081	10081	10081	10081
10082	10082	10082	10082
10083	10083	10083	10083
10084	10084	10084	10084
10085	10085	10085	10085
10086	10086	10086	10086
10087	10087	10087	10087
10088	10088	10088	10088
10089	10089	10089	10089
10090	10090	10090	10090
10091	10091	10091	10091
10092	10092	10092	10092
10093	10093	10093	10093
10094	10094	10094	10094
10095	10095	10095	10095
10096	10096	10096	10096
10097	10097	10097	10097
10098	10098	10098	10098
10099	10099	10099	10099
10100	10100	10100	10100
10101	10101	10101	10101
10102	10102	10102	10102
10103	10103	10103	10103
10104	10104	10104	10104
10105	10105	10105	10105
10106	10106	10106	10106
10107	10107	10107	10107
10108	10108	10108	10108
10109	10109	10109	10109
10110	10110	10110	10110
10111	10111	10111	10111
10112	10112	10112	10112
10113	10113	10113	10113
10114	10114	10114	10114
10115	10115	10115	10115
10116	10116	10116	10116
10117	10117	10117	10117
10118	10118	10118	10118
10119	10119	10119	10119
10120	10120	10120	10120
10121	10121	10121	10121
10122	10122	10122	10122
10123	10123	10123	10123
10124	10124	10124	10124
10125	10125	10125	10125
10126	10126	10126	10126
10127	10127	10127	10127
10128	10128	10128	10128
10129	10129	10129	10129
10130	10130	10130	10130
10131	10131	10131	10131
10132	10132	10132	10132
10133	10133	10133	10133
10134	10134	10134	10134
10135	10135	10135	10135
10136	10136	10136	10136
10137	10137	10137	10137
10138	10138	10138	10138
10139	10139	10139	10139
10140	10140	10140	10140
10141	10141	10141	10141
10142	10142	10142	10142
10143	10143	10143	10143
10144	10144	10144	10144
10145	10145	10145	10145
10146	10146	10146	10146
10147	10147	10147	10147
10148	10148	10148	10148
10149	10149	10149	10149
10150	10150	10150	10150
10151	10151	10151	10151
10152	10152	10152	10152
10153	10153	10153	10153
10154	10154	10154	10154
10155	10155	10155	10155
10156	10156	10156	10156
10157	10157	10157	10157
10158	10158	10158	10158
10159	10159	10159	10159
10160	10160	10160	10160
10161	10161	10161	10161
10162	10162	10162	10162
10163	10163	10163	10163
10164	10164	10164	10164
10165	10165	10165	10165
10166	10166	10166	10166
10167	10167	10167	10167
10168	10168	10168	10168
10169	10169	10169	10169
10170	10170	10170	10170
10171	10171	10171	10171
10172	10172	10172	10172
10173	10173	10173	10173
10174	10174	10174	10174
10175	10175	10175	10175
10176	10176	10176	10176
10177	10177	10177	10177
10178	10178	10178	10178
10179	10179	10179	10179
10180	10180	10180	10180
10181	10181	10181	10181
10182	10182	10182	10182
10183	10183	10183	10183
10184	10184	10184	10184
10185	10185	10185	10185
10186	10186	10186	10186
10187	10187	10187	10187
10188	10188	10188	10188
10189	10189	10189	10189
10190	10190	10190	10190
10191	10191	10191	10191
10192	10192	10192	10192
10193	10193	10193	10193
10194	10194	10194	

LADJIC LINE MODEL OF THE AH-1G HELICOPTER
 UNDAMPED FORCED RESPONSE STRAIN ENERGY METHOD
 PILOT SEAT RESPONSE TO 1000 LR 2/REV VERT HIR SHEAR

ELEMENT TYPE # ELAS1		ELEMENT STRAIN ENERGIES		* TOTAL FOR ALL TYPES # 4.3682823E+00	
				PERCENT OF TOTAL *	
ELEMENT-ID		STRAIN-ENERGY			
41401		4.112961E-04		0.0004	
41462		2.245739E-06		0.0001	
41463		4.110624E-03		0.0009	
42471		4.137592E-04		0.0005	
42472		2.245739E-06		0.0001	
42473		2.164913E-03		0.0006	
42481		4.112961E-04		0.0004	
42482		2.245739E-06		0.0001	
42483		4.112961E-04		0.0004	
44491		1.965863E-06		0.0000	
44492		1.965863E-06		0.0000	
44493		2.764633E-02		0.6329	
45503		1.510120E-01		3.4570	

*** USER WARNING MESSAGE 2350.
 GPFOR MIXTURE IS UNABLE TO CONTINUE AND HAS BEEN TERMINATED DUE TO ERROR MESSAGE PRINTED ABOVE OR BELOW THIS MESSAGE.
 THIS ERROR OCCURRED IN GPFOR CODE WHERE THE VARIABLE -NERROR- WAS SET # 20

APRIL 4 1979 NASTHAN 1/17/77 PAGE 32

ELASTIC LINE MODEL OF THE AH-1G HELICOPTER
UNDAMPED FORCED RESPONSE STRAIN ENERGY METHOD
PILOT SEAT RESPONSE TO 1000 L³ 2/REV VERT HUB SHEAR

*** SYSTEM WARNING MESSAGE 3002
EOF ENCOUNTERED WHILE READING DATA SET SCRATCH3XFILE 303K IN SUBROUTINE GPFDR

SYMBOLS

A	Element cross-sectional area
C	Viscous damping matrix
E	Modulus of elasticity
F	Applied force
G	Complex receptance matrix
I	Element area moment of inertia
K	Stiffness matrix
k	Scalar spring
M	Mass matrix
m	Scalar mass
S	Stiffness ratio
SE	Strain energy
t	Time
x	Structural displacement response vector
Z	Pilot's seat vertical displacement response
δ	Element displacement response vector
ω	Circular frequency of the applied forces
ϕ	Element natural frequency mode shape (eigenvector)
ζ	Element structural damping coefficient

Subscripts

b	Baseline
e	Element
I	Imaginary component of response

j jth element
m At minimum response
n At resonance
R Real component of response

Superscripts

T Matrix transpose

DATE
FILMED

0-8